AFRL-AFOSR-VA-TR-2018-0436

Manipulating Excited State Energy Flow in Organic Systems using Radical Polymers

Bryan Boudouris
PURDUE UNIVERSITY

12/07/2018
Final Report

Air Force Research Laboratory
AF Office Of Scientific Research (AFOSR)/ RTB2
Arlington, Virginia 22203
Air Force Materiel Command

REPORT DOCUMENTATION PAGE

Form Approved
OMB No. 0704-0188

1. REPORT DATE *(DD-MM-YYYY)*	**2. REPORT TYPE**	**3. DATES COVERED** *(From - To)*
11/30/2018	Final Performance Report	15 SEP 2015 - 14 SEP 2018

4. TITLE AND SUBTITLE
Final Performance Report Regarding "Manipulating Excited State Energy Flow in Organic Systems using Radical Polymers"

5a. CONTRACT NUMBER

5b. GRANT NUMBER
FA-9550-15-1-0449

5c. PROGRAM ELEMENT NUMBER

6. AUTHOR(S)
Boudouris, Bryan, W.

5d. PROJECT NUMBER

5e. TASK NUMBER

5f. WORK UNIT NUMBER

7. PERFORMING ORGANIZATION NAME(S) AND ADDRESS(ES)
Purdue University
401 South Grant Street
West Lafayette, IN 47907-2024

8. PERFORMING ORGANIZATION REPORT NUMBER

9. SPONSORING/MONITORING AGENCY NAME(S) AND ADDRESS(ES)
SPONSOR
USAF, AFRL DUNS 143574726
Air Force Office of Scientific Research
875 North Randolph Street, Room 3112
Arlington, VA 22203

10. SPONSOR/MONITOR'S ACRONYM(S)
AFOSR

11. SPONSOR/MONITOR'S REPORT NUMBER(S)

12. DISTRIBUTION/AVAILABILITY STATEMENT
Approved for Public Release; Distribution is Unlimited

13. SUPPLEMENTARY NOTES
This is the Final Progress Report regarding Boudouris' award from 2015. This award was sponsored by the AFOSR, and the award was administered by the Office of Naval Research in the Chicago Regional Office.

14. ABSTRACT
Controlling charge and energy transport in closed-shell conjugated polymers has been a subject of intense study for a number of years; however, implementing a molecular design archetype that includes open-shell (i.e., radical) materials has been extremely limited. Conversely, we demonstrate that the inclusion of radical-containing materials provides significant means by which to manipulate these charge and energy landscape profiles if the macromolecular open-shell designs are synthesized in the appropriate manner. Moreover, these molecular design motifs were evaluated in three end-use applications that are of potential interest to the Department of Defense.

15. SUBJECT TERMS
Organic electronics; Polymer thermoelectrics; Radical polymers; Open-shell dopants; Charge and energy transfer in optoelectronically-active macromolecules; Highly-conductive, transparent plastics

16. SECURITY CLASSIFICATION OF:			**17. LIMITATION OF ABSTRACT**	**18. NUMBER OF PAGES**	**19a. NAME OF RESPONSIBLE PERSON**
a. REPORT	**b. ABSTRACT**	**c. THIS PAGE**			Bryan W. Boudouris
U	U	U	UU	32	**19b. TELEPHONE NUMBER** *(Include area code)* (765) 496-6056

INSTRUCTIONS FOR COMPLETING SF 298

1. REPORT DATE. Full publication date, including day, month, if available. Must cite at least the year and be Year 2000 compliant, e.g. 30-06-1998; xx-06-1998; xx-xx-1998.

2. REPORT TYPE. State the type of report, such as final, technical, interim, memorandum, master's thesis, progress, quarterly, research, special, group study, etc.

3. DATE COVERED. Indicate the time during which the work was performed and the report was written, e.g., Jun 1997 - Jun 1998; 1-10 Jun 1996; May - Nov 1998; Nov 1998.

4. TITLE. Enter title and subtitle with volume number and part number, if applicable. On classified documents, enter the title classification in parentheses.

5a. CONTRACT NUMBER. Enter all contract numbers as they appear in the report, e.g. F33315-86-C-5169.

5b. GRANT NUMBER. Enter all grant numbers as they appear in the report. e.g. AFOSR-82-1234.

5c. PROGRAM ELEMENT NUMBER. Enter all program element numbers as they appear in the report, e.g. 61101A.

5e. TASK NUMBER. Enter all task numbers as they appear in the report, e.g. 05; RF0330201; T4112.

5f. WORK UNIT NUMBER. Enter all work unit numbers as they appear in the report, e.g. 001; AFAPL30480105.

6. AUTHOR(S). Enter name(s) of person(s) responsible for writing the report, performing the research, or credited with the content of the report. The form of entry is the last name, first name, middle initial, and additional qualifiers separated by commas, e.g. Smith, Richard, J, Jr.

7. PERFORMING ORGANIZATION NAME(S) AND ADDRESS(ES). Self-explanatory.

8. PERFORMING ORGANIZATION REPORT NUMBER. Enter all unique alphanumeric report numbers assigned by the performing organization, e.g. BRL-1234; AFWL-TR-85-4017-Vol-21-PT-2.

9. SPONSORING/MONITORING AGENCY NAME(S) AND ADDRESS(ES). Enter the name and address of the organization(s) financially responsible for and monitoring the work.

10. SPONSOR/MONITOR'S ACRONYM(S). Enter, if available, e.g. BRL, ARDEC, NADC.

11. SPONSOR/MONITOR'S REPORT NUMBER(S). Enter report number as assigned by the sponsoring/ monitoring agency, if available, e.g. BRL-TR-829; -215.

12. DISTRIBUTION/AVAILABILITY STATEMENT. Use agency-mandated availability statements to indicate the public availability or distribution limitations of the report. If additional limitations/ restrictions or special markings are indicated, follow agency authorization procedures, e.g. RD/FRD, PROPIN, ITAR, etc. Include copyright information.

13. SUPPLEMENTARY NOTES. Enter information not included elsewhere such as: prepared in cooperation with; translation of; report supersedes; old edition number, etc.

14. ABSTRACT. A brief (approximately 200 words) factual summary of the most significant information.

15. SUBJECT TERMS. Key words or phrases identifying major concepts in the report.

16. SECURITY CLASSIFICATION. Enter security classification in accordance with security classification regulations, e.g. U, C, S, etc. If this form contains classified information, stamp classification level on the top and bottom of this page.

17. LIMITATION OF ABSTRACT. This block must be completed to assign a distribution limitation to the abstract. Enter UU (Unclassified Unlimited) or SAR (Same as Report). An entry in this block is necessary if the abstract is to be limited.

AFOSR Organic Materials Chemistry: Final Performance Report
Grant: FA9550-15-1-0449
September 15, 2015 (Start of Year 1 Performance) – September 14, 2018

Lead Organization: Purdue University
Technical Point of Contact: Professor Bryan W. Boudouris
Administrator Point of Contact: Ms. Helen Moschinger

Proposal Title

Manipulating Excited State Energy Flow in Organic Systems using Radical Polymers

AFOSR Program Manager: Dr. Kenneth Caster

Abstract

Controlling charge and energy transport in closed-shell conjugated polymers has been a subject of intense study for a number of years; however, implementation of a molecular design archetype that includes open-shell (i.e., radical) materials has been extremely limited. Conversely, we demonstrate that the inclusion of radical-containing materials provides significant means by which to manipulate these profiles if the macromolecular open-shell designs are synthesized in the appropriate manner. Moreover, these molecular design motifs were evaluated in three end-use applications that are of potential interest to the Department of Defense. We designed open-shell materials and evaluated their performance as: (1) charge- and energy-accepting moieties from conjugated polymers that had been photoexcited; (2) interfacial modifiers between semiconducting layers and metallic contacts in solar cells and organic field-effect transistors; and (3) dopants for thermoelectric conjugated polymers. Importantly, three overarching themes emerged from this work. First, the mechanism associated with energy transfer between photoexcited conjugated polymers and open-shell additives was established. Second, the design rules for creating radical polymers with high electrical conductivity values was elucidated in full. Third, open-shell dopants offer a means by which to increase the electrical conductivity of conjugated polymers while having minimal impact on the thermopower of the conjugated polymers. Therefore, this is foundational work for an emerging research field (i.e., that of radical-containing organic electronics), and we demonstrated that we can design, synthesize, and manipulate the physical chemistry associated with open-shell species in order to enhance performance in materials and devices of interest to the defense community.

Executive Summary of Research Accomplishments and Technical Achievements

The primary objectives of the grant were threefold, and they were to: (1) elucidate the mechanism of charge and energy transfer between closed-shell conjugated polymers and open-shell (i.e., radical) species; (2) enhance the performance of thin film organic and hybrid electronic devices by inserting a radical polymer interlayer between the semiconducting layer and the metallic electrodes; and (3) utilize radical-containing materials to enhance the electrical conductivity and thermopower of thermoelectric polymers. In short, we have achieved these technical objectives, and the results generated by our team and our research partners have been published or are currently under review in publically-accessible, high-impact journals. In this way, we believe that we have significantly advanced the field of solid-state charge transport in pristine radical polymers and radical-containing organic electronic composites. We note that this field was initially established, in large part, through our initial funding through the Young Investigator Program (YIP). Neither of these efforts would have been possible without the support of the AFOSR, and we thank the agency for these opportunities. Specifically, in this final report, we detail the specific accomplishments of the previous 3 years. In an abbreviated form, these major technical objectives can be summarized as follows. We have:

1. Revealed that the appropriate design of open-shell molecular systems can quench fluorescence emission from common conjugated polymer systems in a highly-efficient manner.
2. Established, through a combination of computation and experimentation, that the fundamental process of this fluorescence quenching procedure is one that follows a Förster resonance energy transfer (FRET) mechanism.
3. Demonstrated that radical-based systems are stimuli-responsive with respect to their optoelectronic properties if the appropriate materials are synthesized. Moreover, we have shown that these materials can act as molecular logic elements through the proper tuning of the molecular chemistry and the redox environment in which the open-shell molecules find themselves.
4. Implemented radical polymers as interlayers in organic field-effect transistors (OFETs) based upon a pentacene active layer. This caused a decrease in the contact resistance between the metallic contacts and the organic semiconductor.
5. Doped common radical polymers with oxidation-reduction-active (redox-active) small molecules in order to increase the solid-state electrical conductivity of the materials by ~5-fold.
6. Copolymerized a crosslinkable moiety into the macromolecular architecture of the radical polymer species in order to provide a transparent conducting polymer that could be crosslinked after spin-coating through exposure to ultraviolet (UV) light. This radical copolymer was then utilized as a charge transporting layer in thin film perovskite solar cells. The insertion of the radical copolymer increased the overall power conversion efficiency of the device from 13.6% to 15.9%.
7. Utilized this radical copolymer as the transparent counter electrode in long-lived electrochromic displays. The cycling stability of these end-use devices highlighted the long lifetimes of radical species and the ability to prevent dissolution of the radical polymer

species into solution even after multiple cycles using relatively harsh organic solvents in the electrochromic device.

8. Synthesized a low-glass transition temperature polymer, and we were the first team to demonstrate that thermal annealing of this new polymer allowed for electrical conductivity values in excess of 20 S m^{-1}. This is a world-record value for radical polymers, and the overall magnitude of this electrical conductivity in pristine (i.e., not doped) non-conjugated polymers places it on par with commodity doped conjugated polymers like certain grades of poly(3,4-etheylene dioxythiophene) doped with poly(styrene sulfonate) (PEDOT:PSS). Moreover, we elucidated the fundamental mechanism as to why this non-conjugated radical polymer was able to achieve such high electrical conductivity values, which set the stage for the development of next-generation radical polymers that have even better charge carrier properties.
9. Manipulated the thermoelectric properties of a common conjugated polymer, poly(3-hexylthiophene) (P3HT), in a selective manner using radical dopants such that the electrical conductivity could be increased substantially without a negative impact on the thermopower of the conjugated moiety. Through appropriate molecular design, the power factor of the thermoelectric materials were increased by ~1,000-fold. This ability to avoid the commonly-observed trade-off in thermoelectric materials could prove vital in transitioning organic thermoelectric systems from the laboratory to the hands of end-users.
10. Created the first open-shell polymer – open-shell small molecule dopant system in order to establish a new materials paradigm in organic thermoelectric materials. These materials displayed one of the highest thermoelectric performance values outside of PEDOT:PSS reported in the literature. This opens a new direction in terms of making long-lasting, humidity-resistant polymer thermoelectric modules for myriad energy conversion applications.

Accomplishing the above objectives has resulted in tangible metrics for this project in terms of the education of postdoctoral scholars and students, increased collaborations with other AFOSR-sponsored university research teams, rapid dissemination of results, and national recognition for our work. In this way, we aim to use these results to positively impact science and technology inside the Department of Defense and across the research community as well. In particular, the support of the AFOSR has allowed the following events to occur over the period of performance for the grant.

1. Two postdoctoral researchers who joined the project in series (i.e., they worked on the project in a back-to-back manner), three graduate students (two self-funded), and one undergraduate student have worked on this project directly. The ability to provide the stipend, benefits, tuition, and materials/supplies of one postdoctoral researcher (at a time) and one graduate student has proven invaluable to the continued success of the laboratory, and we thank the AFOSR for this support. The first postdoctoral researcher who worked on this project is completing a second postdoctoral position at the University of California, Santa Barbara prior to looking for a faculty position. The second postdoctoral researcher has obtained a staff-scientist position at the Korea Institute of Science and Technology (KIST). One of the graduate students is still enrolled in doctoral programs at Purdue University, and he will graduate in 1-2 years. The second graduate student has graduated,

and he is currently a postdoctoral researcher at the University of Delaware. The third graduate student graduated from Purdue, and he is currently continuing his research endeavors at Louisiana State University.

2. Eleven manuscripts have been published during the award period. Furthermore, 3 additional manuscripts are under review currently. Additionally, one patent application has been submitted based upon this work. We note that all publications have recognized the support of the AFOSR in the Acknowledgements sections of the manuscripts. We anticipate that the three manuscripts that are still under review will be published in the near future. Thus, 14 total manuscripts will be published during the 3-year period of performance from this grant. The published manuscripts are the following.

    a. "Recent Advances in the Syntheses of Radical-Containing Macromolecules," Wingate, A. J.; Boudouris, B. W. *J. Polym. Sci. Part A: Polym. Chem.* **2016**, *54*, 1875–1894.

    b. "Radical Polymers Improve the Metal-Semiconductor Interface in Organic Field-Effect Transistors," Sung, S. H.; Bajaj, N.; Rhoads, J. F.; Chiu, G. T.; Boudouris, B. W. *Org. Electron.* **2016**, *37*, 148–154.

    c. "Impact of the Addition of Redox-Active Salts on the Charge Transport Ability of Radical Polymer Thin Films," Baradwaj, A. G.; Wong, S. H.; Laster, J. S.; Wingate, A. J.; Hay, M. E.; Boudouris, B. W. *Macromolecules* **2016**, *49*, 4784–4791.

    d. "Organic Radical Polymers: New Avenues in Organic Electronics," Mukherjee, S.; Boudouris. B. W. **2017**, Springer Publishing, New York, NY.

    e. "Design of a Three-State Switchable Chromogenic Radical-based Moiety and Its Translation to Molecular Logic Systems," Mukherjee, S.; Boudouris, B. W. *Mol. Syst. Des. Eng.* **2017**, *2*, 159-164.

    f. "Enhancing Polymer Thermoelectric Performance using Radical Dopants," Tomlinson, E. P.; Mukherjee, S.; Boudouris, B. W. *Org. Electron.* **2017**, *51*, 243-248.

    g. "Radical Polymers as Interfacial Layers in Inverted Hybrid Perovskite Solar Cells," Zheng, L.; Mukherjee, S.; Wang, K.; Hay, M. E.; Boudouris, B. W.; Gong, X. *J. Mater. Chem. A* **2017**, *5*, 23831.

    h. "Stable Radical Materials for Energy Applications," Wilcox, D. A.; Agarkar, V.; Mukherjee, S.; Boudouris, B. W. *Ann. Rev. Chem. Bio. Eng.* **2018**, *9*, 083945.

    i. "A Nonconjugated Radical Polymer Glass with High Electrical Conductivity," Joo, Y.; Agarkar, V.; Sung, S. H.; Savoie, B. M.; Boudouris, B. W. *Science* **2018**, *359*, 1391-1395.

    j. "Thermoelectric Performance of an Open-Shell Donor-Acceptor Conjugated Polymer Doped with a Radical-Containing Small Molecule," Joo, Y.; Huang, L.;

Eedugurala, N.; London, A. E.; Kumar, A.; Wong, B. M.; Boudouris, B. W.; Azoulay, J. D. *Macromolecules* **2018**, *51*, 3886-3894.

k. "Highly Transparent Crosslinkable Radical Copolymer Thin Film as the Ion Storage Layer in Organic Electrochromic Devices," He, J.; Mukherjee, S.; Zhu, X.; You, L.; Boudouris, B. W.; Mei, J. *ACS Appl. Mater. Interfaces* **2018**, *10*, 18956-18963.

The manuscripts that are currently under review are the following.

l. "Molecularly Engineered Organic-Inorganic Hybrid Perovskites Quantum Wells," Gao, Y.; Shi, E.; Snaider, J. M.; Shiring, S. B.; Liang, C.; Liebman-Pelaez, A.; Yoo, P.; Deng, S.; Zeller, M.; Boudouris, B. W.; Liao, P.; Zhu, C.; Yu, Y.; Savoie, B. M.; Huang, L.; Dou, L. **2018**, *submitted for review to Nature Chemistry*.

m. "Tuning the Interfacial and Energetic Interactions between a Photoexcited Conjugated Polymer and Open-Shell Small Molecules," Wilcox, D. A.; Snaider, J.; Mukherjee, S.; Yuan, L.; Huang, L.; Savoie, B. M.; Boudouris, B. W. **2018**, *submitted for review to Soft Matter*.

n. "Radical Polymers Alter the Carrier Properties of Semiconducting Carbon Nanotubes," Joo, Y.; Mukherjee, S.; Boudouris, B. W. **2018**, *submitted for review to ACS Applied Polymer Materials*.

The patent application that is currently under review is the following.

o. "Novel Radical Polymer Film with High Electrical Conductivity," Boudouris, B. W.; Savoie, B. M.; Joo, Y.; Agarkar, V.; Seung, S. H. Filed: July 24, 2018, Under Review with Application Number: 62702377.

3. Support from the AFOSR grant also has allowed our work to be presented, through invited (and contributed) talks, across the globe. We note that all presentations have recognized the support of the AFOSR. The following 22 <u>invited presentations</u> were delivered during the period of performance.

a. "Charge Transport Physics of Non-conjugated Glassy Radical Polymer Conductors." Physical Aspects of Polymer Science Meeting of the Institute of Physics (IOP). September 10, 2015.

b. "Solid-State Charge Transport in Redox-Active Radical Polymers." 228th Electrochemical Society (ECS) Meeting. October 14, 2015.

c. "Designing Macromolecules for Advanced Energy Conversion and Separations Applications." Massachusetts Institute of Technology, Program in Polymers and Soft Matter. October 21, 2015.

d. "Tuning the Thin Film Self-Assembly of Radical-Containing Diblock Copolymers." 2015 AIChE Annual Meeting. November 11, 2015.

e. “Design of Functional Polymers for Advanced Energy Conversion and Water Purification Applications.” University of Illinois at Urbana Champaign, Department of Chemical and Biomolecular Engineering. November 19, 2015.

f. “Designing Macromolecules for Advanced Energy Conversion and Separations Membrane Applications.” 3M Corporation. December 10, 2015.

g. “Self-assembly of Open Shell-Containing Block Polymer Thin Films.” American Physical Society (APS) March Meeting. March 15, 2016.

h. “Making Glasses Conduct: Electrochemical Doping of Redox-Active Polymer Thin Films.” American Physical Society (APS) March Meeting. March 17, 2016.

i. “Correlating Structure with Charge Transport in Radical Polymers.” Polymer Physics Gordon Research Conference (GRC). July 27, 2016.

j. “Manipulating the Solid-state Charge Transport of Radical Polymer Glasses.” Note Dame-Purdue Symposium on Soft Matter and Polymers. October 8, 2016.

k. “Designer Macromolecules for Next-Generation Flexible Electronic and Membrane Adsorber Applications.” BASF Committee for Scientific Innovation and Interaction Seminar Series. October 11, 2016.

l. “Designing Functional Macromolecules for Water Purification and Electronic Applications.” University of Akron, Department of Polymer Science. October 14, 2016.

m. “Solid State Transport in Radical Polymer Glasses and Their Application to Organic Electronic Devices.” 2016 AIChE Annual Meeting (Area 8A (Polymers) Plenary Lecture Session). November 14, 2016.

n. “Designer Polymers for Next-Generation Flexible Electronic and Water Purification Applications.” University of Wisconsin – Madison, Department of Chemical and Biological Engineering. December 13, 2016.

o. “Designing Functional Macromolecules for Water Purification and Electronic Applications.” Tufts University, Department of Chemical and Biological Engineering. February 23, 2017.

p. “Elucidating Solid-State Charge Transfer in Radical Polymers.” American Chemical Society (ACS) PanPoly Conference. March 23, 2017.

q. “Elucidating Charge Transport in Radical-Containing Polymers and the Application to Energy Conversion Devices.” Soft Materials Summer School hosted by the University of Freiburg (Germany). July 6, 2017.

r. “Designing Functional Macromolecules for Electronic Applications and Water Purification.” Purdue-University – Korea University Workshop at the 2017 AIChE Annual Meeting. October 29, 2017.

s. "Designing Functional Polymers for Water Purification and Flexible Electronic Applications." University of Illinois at Chicago, Department of Chemical Engineering. February 13, 2018.

t. "Designing Charge Neutral, Non-Conjugated Radical Polymers with High Electrical Conductivity Values." 2018 ACS Spring Meeting. March 21, 2018.

u. "The Nanoscale Features that Allow Non-conjugated Radical Polymer Glasses to Achieve High Electrical Conductivity Values." 4th Functional Polymeric Materials Conference. June 8, 2018.

v. "Designing Functional Polymers for Water Purification and Flexible Electronic Applications." University of Pittsburgh, Department of Chemical and Petroleum Engineering. October 26, 2018.

4. In addition to these tangible products, the AFOSR-supported work has also brought a number of national and international accolades to the group during the 2015-2018 time period. For instance, Boudouris was invited to deliver the APS Division of Polymer Physics – UK Polymer Physics Group Lectureship in Manchester, UK at the outset of the grant. Moreover, he was inducted into the Purdue Innovators Hall of Fame in 2015 for his work with radical polymers. Also, the group's efforts regarding the stability of radical polymers were featured in the 2018 "Young Talents in Polymer Science" Issue of *Macromolecular Chemistry and Physics*, and they will be recognized again in the 2019 "Emerging Investigators" Issue of *Soft Matter*. All of these recognitions led to Boudouris being recognized with the Purdue College of Engineering Early Career Research Award in 2018. Clearly, none of these recognitions would have been possible without the extraordinary interactions and support of Drs. Lee and Caster and the entire AFOSR team. We thank the program managers and the AFOSR for this mentoring and support during the early stages of our career.

By focusing on the fundamental properties of open-shell systems, we have been able to make significant strides in a number different arenas. In addition to performing work in our laboratory, we also have been able to team successfully with other groups from the Organic Materials Chemistry program in order to produce a number of cross-disciplinary products. In particular, we have teamed with both the group of Professor Xiong Gong at the University of Akron and Professor Jason Azoulay at the University of Southern Mississippi. We are grateful for these experiences, and we hope that we are able to keep these collaborations strong while building new collaborations with partners from other universities and from the laboratories (e.g., the Air Force Research Laboratory). Of course, none of this would have been possible without the support and guidance of the Air Force Office of Scientific Research and our specific program manager, Dr. Kenneth Caster. We are extremely appreciative of the support and mentoring that he has provided during the period of performance. Moreover, we are grateful for the mentorship provided by Dr. Charles Lee who guided this work during the first year of the period of performance. Through their mentoring and support, we have made significant strides in terms of the design, synthesis, and application of radical polymers and radical-containing small molecules. In this way, we aim to have an impact both on the scientific community and also develop means by which we can extend these fundamental discoveries into translatable technologies in order to enable the warfighter to continue to have a distinct advantage in defense situations.

Detailed Research Results for the Entire Period of Performance

Introduction

Radical polymers are an emerging class of charge-conducting macromolecules that have been used in a variety of electrolyte-supported (e.g., flexible battery) applications. However, the fundamental properties, and thus ultimate performance limits, of these materials as charge carriers in the solid state had not been examined until our previous work with the AFOSR. After establishing the ability of these non-conjugated, amorphous (i.e., glassy) polymers to transport charge in a relatively efficient manner in the solid state during our AFOSR YIP funding, we have shifted our attention to utilizing these materials as a means by which to manipulate the flow of charge and energy in organic electronic systems. Fortunately, the open-shell nature of the radical polymers allows for the rather facile manipulation of these parameters. Moreover, the fact that the electronic functionality of the radical polymers is decoupled from the macromolecular backbone chemistry (which mainly controls the mechanical and thermal properties of radical polymers) allows for the team to easily manipulate the transport properties (e.g., the effective work function) of the radical polymers and small molecules. Moreover, this flexibility allows these materials to be utilized in a number of relevant organic electronic device test bed scenarios. Therefore, this work both probes the fundamentals associated with polymer chemistry and polymer physics while also providing clear pathways by which to translate this technology out of the laboratory and into devices of interest to the Department of Defense. Specifically, we have been able to identify three specific topic areas in which radical-containing materials have the opportunity to play significant roles in the future. The first is that of pairing open-shell molecules with photo-excited conjugated polymers in order to observe charge and energy transfer. The second deals with the utilization of radical polymers as interfacial modifiers in a suite of different organic electronic devices. Additionally, this work allowed us to modify the chemical signature of the radical polymers in order to produce a non-conjugated, pristine (i.e., not doped), amorphous, and transparent macromolecular conductor that had an electrical conductivity of > 20 S m^{-1}. Third, we have devised means by which to incorporate radical groups into thermoelectric materials in order to significantly increase the electrical conductivity of conjugated polymers while only slightly negatively impacting the relatively large Seebeck coefficient associated with these materials. In this way, composite open-shell–closed-shell polymer composites were generated with thermoelectric performance values that rival many of the state-of-the-art materials in this field. Importantly, the details of the three thrusts described below highlight that the impressive performance values reached were obtained due to a fundamental understanding of the molecular-level phenomena at play. In this way, we aim to have this work be a source of definitive structure-property-performance relationships such that our team and others can build from this effort in the future.

Thrust 1: Manipulating Excited States in Organic Electronic Chromophores

Stable organic radicals, which contain one or more unpaired electrons in their molecular structure, can undergo oxidation or reduction to form stable ionic species. Therefore, charge can be transferred to (or from) individual radical sites and transported within specific domains of these materials through electron self-exchange reactions in the solid state. As with conjugated materials, radicals are classified based upon whether they are preferentially oxidized (p-type) or reduced (n-type). Materials capable of readily undergoing both types of redox reactions (i.e., to form either a

cationic or anionic species) are referred to as ambipolar. In recent years, the potential value of these radical-based materials has been demonstrated through conducting polymer applications and with their utilization as active interfacial-modifying layers in organic and perovskite solar cells, organic field-effect transistors, and as dopants in thermoelectric applications. Additionally, the non-zero spin of the stable radical species makes them excellent candidates for applications where manipulation of the spin states within a given system are desired. While radical-based materials are now being used in conjunction with conjugated polymers, the fundamental interactions and energy transfer events in these closed-shell–open-shell hybrid composites have not been well illustrated in the literature. In order to more effectively establish the potential application space of this emerging class of materials, the interfacial and energetic interactions between conjugated materials and radical-based materials must be deciphered in full.

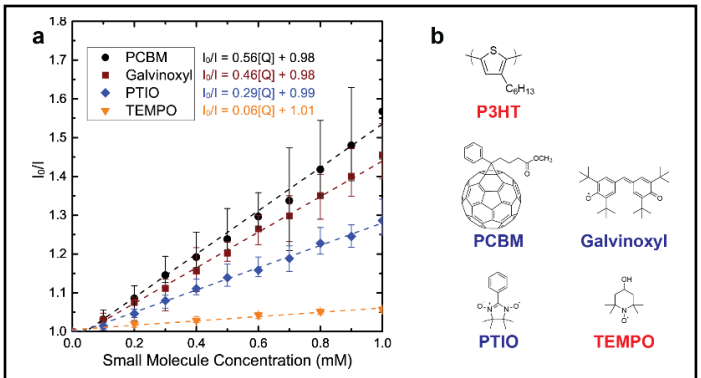

Figure 1. (a) Stern-Volmer plots of the corrected fluorescence intensity of P3HT solutions in chloroform (60 μM of thiophene repeat units) and small molecules that serve as quenching sites for the photoexcited P3HT. The excitation and emission wavelengths for all of the measurements were 500 nm and 578 nm, respectively. (b) Molecular structures of species used in this work. Electron-donating (p-type) species are indicated in red, while electron-accepting (n-type) species are indicated with blue labels.

Specifically, the behavior of the excited states in conjugated polymer systems can be elucidated by evaluating the fluorescent behavior of the macromolecules. In a system of two different molecular species, the quenching of fluorescence is a direct reflection of the intermolecular interactions of the pair. Coincidentally, most non-conjugated radical species are non-fluorescent, owing to their open-shell electronic structure, which facilitates non-radiative decay of their excited states. However, recent studies have demonstrated that fluorescent radical species containing conjugated units exist, and these materials are being actively researched for utilization in OLEDs as their emission from doublet excited states elegantly avoids the 75% loss in quantum efficiency caused by formation of triplet excited states in conventional closed-shell materials. Nevertheless, the vast majority of stable open-shell materials are non-fluorescent. Based on this concept, open-shell moieties such as the 2,2,6,6-tetramethylpiperidine-1-oxyl (TEMPO) radical have often been used as fluorescence quenchers for a variety of soft materials including both conjugated small molecules and quantum dots. In these studies, a variety of mechanisms, including electron transfer, resonance energy transfer, and enhanced intersystem crossing, have been proposed. Here, we establish the principal molecular interactions by which fluorescence quenching between a radical species and a specific conjugated polymer, poly(3-hexylthiophene) (P3HT) occurs, as P3HT has served as an oft-used material in many organic electronic applications. Through a combination of experiment and simulation, we demonstrate that Förster Resonance Energy Transfer (FRET) is the primary mechanism by which the fluorescence quenching occurs in P3HT for radical species that absorb light strongly within the visible range, and that radical species with low optical absorption coefficients do not show significant quenching behavior. Thus, certain interactions become improbable, which allows for the strategic design of systems that utilize both conjugated and radical species. This key point has

significant implications in the development of coupled closed-shell conjugated polymer-radical molecule systems and interfaces with tunable directional energy transport.

Fluorescence quenching activity was observed to a variable degree for some, but not all, of the interacting radical-polymer blends evaluated. Figure 1 shows a Stern-Volmer plot of the fluorescence intensity of solutions of P3HT and the various radical quencher species versus the concentration of the quencher. For comparison, a solution mixture of P3HT and [6,6]-phenyl-C_{61}-butyric acid methyl ester (PCBM) is included, as PCBM acts as an efficient fluorescence quencher for a wide variety of conjugated polymers, including polythiophenes. All solution intensities were corrected for the inner filter effect due to the significant absorption of the quencher species. The quenching behavior for the galvinoxyl radical is on par with that demonstrated by PCBM, suggesting that the galvinoxyl radical is an effective fluorescence quencher for P3HT. PTIO also shows significant quenching behavior, while TEMPO shows insignificant quenching behavior at the concentrations probed. In particular, PCBM shows a Stern-Volmer constant of 0.56 mM^{-1}, the galvinoxyl radical shows one of 0.46 mM^{-1}, the PTIO radical shows one of 0.29 mM^{-1}, and the TEMPO radical shows one of 0.06 mM^{-1} (Figure 1).

A similar trend in relative quenching behavior is seen for thin film composites of P3HT blended with the quencher species (Figure 2). This suggests that a similar mechanism is responsible for the quenching behavior in both solution and film, allowing the nature of the quenching interaction to be examined from both experimental platforms. Absorbance data were used to ascertain the underlying nature of the quenching interaction in these soft materials systems. As can be seen from Figure 3, there is no apparent shift in the absorbance peaks and an absence of the appearance of any new peaks. This is seen in solution phase as well, and in those measurements, the total absorbance follows the Beer-Lambert law for the absorbance of the quencher species in a P3HT solution. That is, the final curve is the sum of the two independent absorption spectra, whose magnitude at all points is proportional to the concentration of species present. This suggests that the quenching observed is a dynamic quenching mechanism and not due to the formation of a non-fluorescent supramolecular complex. A blue shift in the peak near 500 nm for P3HT is visible upon the addition of PCBM, which suggests that PCBM is disrupting the crystalline packing of the P3HT in the solid state.

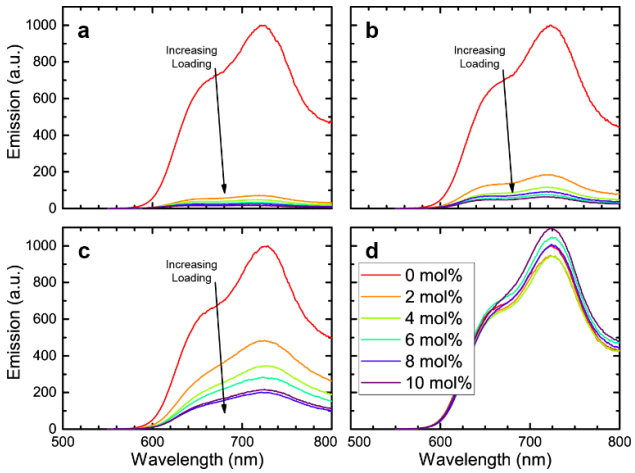

Figure 2. Reduction in intensity of fluorescence spectra of P3HT thin films with increasing loadings of (a) PCBM, (b) the galvinoxyl radical, (c) the PTIO radical, and (d) the TEMPO radical. As with the solution-state measurements, the PTIO and galvinoxyl radicals show a reduction in the P3HT fluorescence intensity in the solid state while the TEMPO radical does not. The excitation wavelength was 500 nm

Interestingly, this peak shift is not observed in any of the P3HT-radical blends. This is consistent with x-ray diffraction (XRD) measurements, which show that the P3HT and the radical species arrange themselves into different crystalline domains at the nanoscale. For the P3HT-

radical blends, the (100) and (010) peaks remain in the same location, suggesting that the P3HT crystalline structure is unaffected by the presence of the radical species. A P3HT-PCBM blend, by contrast, shows a suppression of the (010) peak for P3HT with no appearance of the PCBM crystal peaks, which also suggests that PCBM disrupts the crystalline packing of the P3HT, but does not form its own phase at these low loadings of the quenching species.

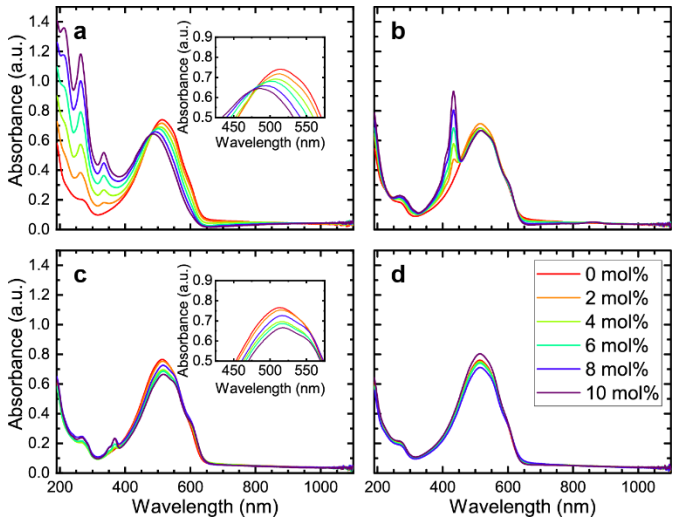

Figure 3. Absorbance spectra of P3HT thin films with increasing amounts of (a) PCBM, (b) the galvinoxyl radical, (c) the PTIO radical, and (d) the TEMPO radical. These data demonstrate that no supramolecular complexes are forming in the ground state between P3HT and the radical species, as the peak locations for P3HT and the radical species are unchanged. Moreover, there is no appearance of a lower energy absorption band. PCBM, by contrast, shows a blue-shifting in the P3HT absorption peak, most likely because the PCBM disrupts the crystalline packing of the P3HT. The insets show the blue-shift for P3HT-PCBM in greater detail, as compared to P3HT-PTIO, which shows no blue-shift.

These trends in quenching data and nanoscale structure are consistent with one of two interaction mechanisms: either (1) photoinduced charge transfer or (2) excited state transfer through a Förster Resonance Energy Transfer (FRET) pathway. Both the galvinoxyl and PTIO radicals show significant absorbance coefficients within the region of the spectrum where P3HT emits, both in solution phase and in solid state (Figure 4). TEMPO, by contrast, shows minimal absorbance in that region. This spectral overlap suggests that FRET may be the mechanism for the observed quenching. However, the observed trend in quenching behavior is also consistent with photoinduced electron transfer as a mechanism. In thin films, the fluorescence quenching of P3HT by PCBM is caused by such a mechanism, and based upon the observed redox behavior of the radical species, a photoinduced electron transfer mechanism is energetically viable. The galvinoxyl and PTIO radicals show a reduction potential of 4.7 and 4.1 eV below vacuum, respectively. These values are farther-removed from vacuum than that of the lowest unoccupied molecular orbital (LUMO) energy of P3HT, which is 3.0 eV below vacuum, indicating that an electron transfer from an excited P3HT to one of these radical species could occur (inset of Figure 4). The TEMPO radical, by contrast, has never been observed to form a stable anion species, suggesting that it would be unable to act as an electron acceptor. As both mechanisms are consistent with the observed trend, further characterizations are necessary to quantify the relative importance of the different mechanisms.

To uncover which mechanisms are at play in these optoelectronically-active blends, transient absorption spectra of the P3HT-radical blends were compared with the spectrum of pristine P3HT (Figure 5). The spectrum of pristine P3HT shows a bleach signal between 500 and 600 nm, corresponding to the ground-state bleach (GSB), as well as a photoinduced absorption between 600 and 700 nm, corresponding to photoinduced absorption of delocalized polarons (i.e.,

positively-charged P3HT segments within crystalline regions of the thin film). Comparing this spectrum with the spectra associated with those of the P3HT-radical blends shows little qualitative difference. That is, no additional signals corresponding to bleaching of the radicals or photoinduced absorption of their anions can be detected. In the case of the galvinoxyl radical, the main absorbance peak is found at 400 nm, outside the range of the detector. The galvinylate anion, however, absorbs strongly at 560 nm, well within the range measured. No clear difference can be seen between the spectra at this point, suggesting that photoinduced charge transfer is not at play, despite the energetic favorability of such a transfer. In the case of PTIO, the main absorbance peak overlaps with that of P3HT, and the anion absorbs around 325 nm, also outside the range that can be measured by the available equipment. Nevertheless, a clear difference is seen between the P3HT-radical blends and the P3HT-PCBM blend, which does show charge transfer. A larger polaron signal is present, and the signal persists for the entire measurement, which is consistent with photoinduced charge separation. The lack of similar signals suggests that charge transfer is not occurring in the P3HT-radical blends. The data in the time domain reveal a clear difference in behavior between the pristine P3HT and the P3HT-radical composite films. For the P3HT-radical blends, both the GSB and the polaron signals decay significantly more rapidly than for the pristine film, suggesting that the radicals enhance the rate of ground state recovery. This is in stark contrast to the P3HT-PCBM film, where the ground state bleach and polaron signals persist with minimal decay through the duration of the experiment, due to the long-term charge separation. Additionally, the dynamics of the GSB and polaron signals appear to track each other well for both the pristine and radical-doped films, which suggests that the presence of the radicals has little effect on the formation of polarons within the film. This clear contrast between P3HT-PCBM and the radical signals, as well as the absence of any signals corresponding to the anions of the radical acceptors within the wavelength window probed, suggests that charge transfer is minimal in these blends. However, the increased rate of decay for the GSB is consisted with FRET as a mechanism, as resonant energy transfer results in regeneration of the ground state of the donor. Therefore, FRET appears to be the dominant mechanism behind the observed fluorescence quenching.

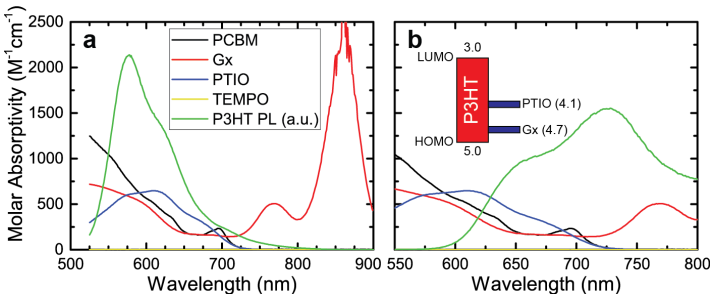

Figure 4. Overlap of the P3HT emission spectrum (green line) with the absorbance spectra of the quencher molecules. (a) The emission spectrum of a 60 μM P3HT solution in chloroform, and (b) the emission spectrum of a P3HT thin film. The inset shows the frontier orbital (HOMO and LUMO) energies of P3HT and the reduction potentials, in units of eV removed from free vacuum, of the two n-type open-shell species: the PTIO and galvinoxyl radicals.

In conclusion, the electronic and energetic interactions between open-shell small molecules and a common conjugated polymer, P3HT, in solution and as composite thin films were evaluated in full. Specifically, the fluorescence of P3HT was observed to be effectively quenched by the stable organic open-shell species, the galvinoxyl and PTIO radicals both in solution and as thin films, with quenching performance on par with that of PCBM. The TEMPO radical, by contrast, showed minimal quenching of the P3HT fluorescence. As demonstrated through a combination of computation (results not shown here), steady-state spectroscopy, and ultrafast spectroscopy, the quenching behavior was primarily due to resonant energy transfer between the two species, in

contrast to the electron-transfer mechanism that is dominant in the classic closed-shell quencher PCBM. This mechanism was supported by the large spectral overlap between the absorbance spectra of the radical species that acted as quenchers and the emission spectrum of the P3HT donor, as well as the rapid recovery of the ground state observed through transient absorption measurements. Charge transfer, an alternative plausible mechanism, was determined to not be the primary means of fluorescence quenching in the P3HT-radical systems evaluated here as the signal of the quencher anions were not observed in the transient absorption, as well as through calculations that suggested it would proceed at a far slower rate than through FRET. As FRET is a long range interaction, this finding has implications for future applications involving energy transfer from a fluorescent conjugated molecule to an open shell species, such as heterojunctions between the two in device applications or in conjugated molecules bearing radical pendant groups. Specifically, the finding suggests that by choosing a radical species that can act as a FRET acceptor for a given conjugated species, greater flexibility in the distance between the two moieties can be achieved. Moreover, it highlights the key need to appropriately and fully evaluate the subtle physical, electronic, and energetic interactions between closed-shell and open-shell organic composite materials. Because of this important insight regarding the responsivity of the galvinoxyl radical relative to other radical species, we turned our focus to the galvinoxyl-based radicals in order to better understand the redox and optoelectronic properties of this important class of open-shell systems.

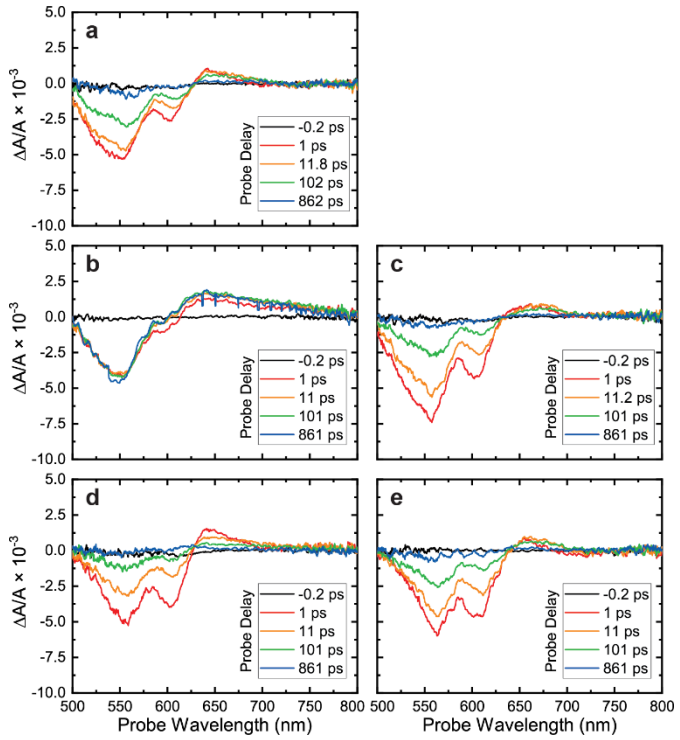

Figure 5. Representative transient absorption spectra of a (a) pristine P3HT film, (b) P3HT-PCBM blend, (c) P3HT-Galvinoxyl blend, (d) P3HT-PTIO blend, and (e) P3HT-TEMPO blend at selected delay times. The negative signal from 500 to 625 nm corresponds to the ground-state bleaching of the P3HT film, while the positive signal from 625 to 700 nm corresponds to delocalized polarons in the P3HT film. The pump wavelength was 400 nm.

Specifically, we established the stimuli-responsive behavior of a galvinoxyl radical-containing monomer and polymer, poly(galvinoxyl styrene) (PGSt). The closed-shell monomer, 2,6-di-tert-butyl-4-((3,5-di-tert-butyl-4-hydroxyphenyl) (4-vinylphenyl)methylene) cyclohexa-2,5-dien-1-one (GStH), was synthesized according to a four step process that utilized a 2,4-di-tert-butyl phenol starting material. The presence of the vinyl group in GStH is such that it can be used to polymerize the molecule, forming PGStH (Figure 6). These two chemical species can be oxidized (using $K_3[Fe(CN)_6]$ in the presence of NaOH) to form the corresponding radical species. Thus, combining the deprotonated (GStB/PGStB) and the radical state (GSt/PGSt), the system has

three unique identities that have key differences in the symmetry and the number of π-electrons in the conjugated backbone. The half-phenolic and half-quinoidal neutral structure (GStH) is asymmetric and weakly conjugated compared to the other two species. Although GStB and GSt are structurally identical in terms of molecular design, they are electronically dissimilar. Importantly, the three distinct species (i.e., closed-shell neutral, conjugate-base anion, and radical) are distinctly different in color. Where GStH is orange, the color of GSt is darker brown. With only one more electron in the system, the anionic GStB is clearly different, and it appears as a much darker blue material. Such a different appearance of the conjugate-base (GStB) constitutes what is known as a halochromic behavior in the material. Beyond this halochromic behavior being of fundamental chemical import, the distinct optical signatures of the species allow for the facile monitoring of the interplay and conversion of the three different species, which provided a more detailed insight into the formation mechanism and stability of the radical species, as both a small molecule as well as a polymer.

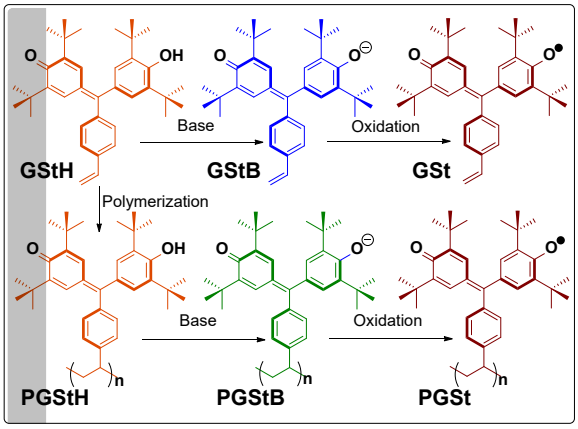

Figure 6. Molecular formulae and reaction interplay between GSt, GStH and GStB (top). Similarly, the same structures for the polymeric systems (PGSt, PGStH and PGStB) are shown in the lower portion of the figure. The colors represent the visual appearances of the species when dissolved in aqueous solution.

As depicted in Figure 7, GStH shows a moderately strong and structurally broad absorption band at 415 nm ($\varepsilon = 1.0 \times 10^4$ $M^{-1}cm^{-1}$) and additional higher energy absorption bands as well. Density functional theory (DFT) computations indicated that the frontier molecular orbitals (FMOs) of the compound are dominated by the quinonoid side of the system, and the computed transition ($\lambda = 426$ nm, $f = 0.614$; f represents computed oscillator strength) is predominantly a HOMO-LUMO transition dominated by the quinonoid moiety. On gradual deprotonation, the formation of GStB is clearly observable due to the formation of a much stronger absorption band near 600 nm ($\varepsilon = 1.5 \times 10^4$ $M^{-1}cm^{-1}$). Computational assessment also agrees closely with the experimental observation, and predicts a HOMO-LUMO transition at $\lambda = 632$ nm ($f = 0.682$). The symmetric disposition of the FMOs, coupled with the increased conjugation through the overall π-conjugated system, results in a lowered band gap of the compound. Further, the higher oscillator strength of the HOMO-LUMO transition can be correlated to the stronger absorption features of GStB. In addition, due to formation of a symmetric but rigid conjugated structure, the absorption profile for GStB is comparatively narrower than the neutral form. Apart from the dominant absorption band at 600 nm, GStB also shows two distinct peaks at 310 nm and 390 nm, which can be ascribed to localized π-π* transitions. Upon oxidation (in aqueous solution) of GStB to GSt, the dominant absorption peak at 600 nm disappears with the formation of a new distinct peak at 485 nm ($\varepsilon = 0.9 \times 10^4$ $M^{-1}cm^{-1}$). Additionally, a number of higher energy absorption bands were observed. The formation of the radical species could be also confirmed from the characteristics peaks of GSt observed using cyclic voltammetry (*in situ*). Interestingly, the removal of one electron from GStB, decreases the relative energies of the FMOs However, the filled orbital (i.e.,

the simultaneous HOMO/SOMO) experiences a more significant lowering (compared to the virtual LUMO), which effectively increases the HOMO-LUMO gap with a lower oscillator strength (λ = 461 nm, f = 0.533), according to computations. Considering the structure and electronic properties of the conjugate-base (GStB) and radical (GSt), it is evident that the relative torsional orientations of the three aromatic rings in the two species are comparable. However, the bond lengths in the conjugate base structure are comparatively elongated, which again supports the previously discussed argument of electronic repulsion in the system. It is notable that, similar to the FMOs, the electrostatic potential surface is also symmetric in GStB and GSt. However, in GSt, the spin density is only localized symmetrically on the two phenolic aromatic rings, which is comparable to the galvinoxyl radical. Thus, the third styryl ring has an insignificant effect on controlling the electronic properties of GSt.

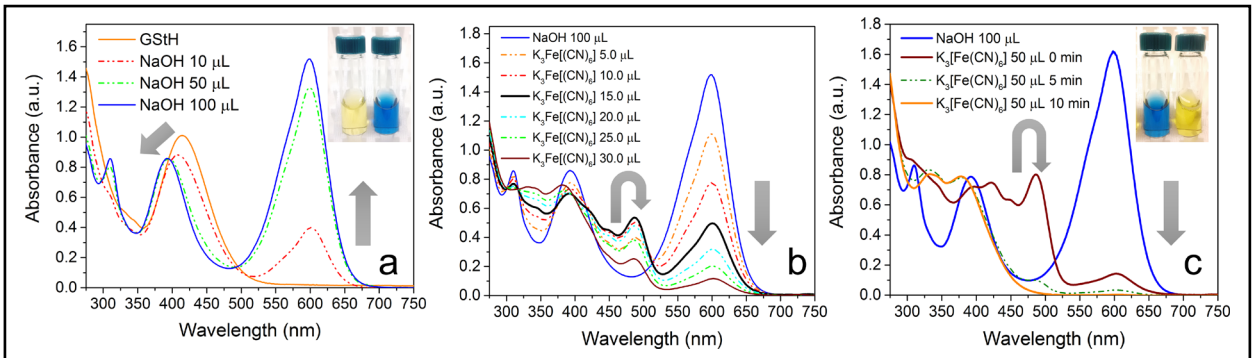

Figure 7. (a) Changes in the UV-Vis absorption profile of GStH (3 mL, 0.1 mM in 1:9 THF-H_2O mixture) upon titration against NaOH (0.1 g mL^{-1}). The emergence of the new peak at 600 nm is due to formation of GStB, which visually changes the color of the solution to dark blue (inset). (b) Reaction of the generated GStB with the gradual addition of $K_3[Fe(CN)_6]$ (10 mM) shows the formation of a new distinct peak at 485 nm. However, the maximum intensity of this peak is observed at the middle of the titration, which indicates that the formed species in unstable in presence of NaOH (aq). (c) The unstable nature of GSt in NaOH (aq) is demonstrated. Addition of excess $K_3[Fe(CN)_6]$ at a single time results in nearly 90% conversion to the radical species; however, a gradual decomposition of this radical species subsequently follows. The inset picture shows the immediate disappearance of the blue color of GStB upon addition of $K_3[Fe(CN)_6]$.

Apart from the fundamental optical properties, the distinct color signals of the radical (GSt) compared to the anionic species (GStB) reveals the formation mechanism of radical polymers (e.g., PGSt). Observation of a maximum intensity (at λ = 485 nm) during the course of the addition of $K_3[Fe(CN)_6]$ pointed towards the relative instability of GSt in aqueous media. In fact, it can be observed more prominently via the addition of excess $K_3[Fe(CN)_6]$ to GStB in one batch and the subsequent monitoring of the optical profile at 485 nm as a function of time. The partial deprotonation of the available GStH in aqueous media still leads to the formation of, and increases the stability of, GSt. It is notable that the decrease in the concentration of GStB is rapid relative to the formation of GSt, indicating that the deprotonation might be the rate-determining step in formation of the radical species. This is further supported in the case of the PGSt polymer as well. The neutral monomer (GStH) can be polymerized using free radical polymerization. However, due to the steric bulk of the system, only macromolecules with moderately low molecular weights (M_n = 4.1 kg mol^{-1}) were obtained, which corresponded to ~10 repeat units. In a manner akin to the small molecule (GStH), the polymer, PGStH, also shows a significant extent of deprotonation in basic solvents. In order to establish the structural orientation of the polymer, we optimized the geometry of small chain models (12 repeat units) computationally, and determined that the chains

should adopt a helical shape. As demonstrated in Figure 8, the phenolic units are placed towards the periphery of the helix, which has a threefold screw-symmetry. Thus, it is expected that the -OH sites are solvent accessible (unlike the π-conjugated systems of the repeating units), and the core alkyl chain is shielded by bulky aromatic substituents. Significantly, the addition of even excess base to an aqueous solution of PGStH (in THF/H_2O) results in only ~15% of the possible deprotonation after which the material starts to precipitate. Thus, even with the pendant sites being solvent accessible, it appears that only single deprotonation occurs in each polymer chain. After this point the macromolecular solubility is compromised in the solvent mixture. Interestingly, such partial progress of the reaction imparts a green color to the mixture of yellow- and blue-colored materials. Comparing soaked filter paper strips of GStH and PGStH and their exposure to purely aqueous NaOH demonstrates a similar behavior. However, this observation indicates that the partial deprotonation of PGStH is probably due to the inability of the material to form poly-anionic species, which may result in significant electronic repulsions between proximal repeat units along the same macromolecular backbone. Thus, even with the presence of similar functional units, a monomer and a polymer can have distinctly distinguishable halochromic features. Such modulation of the color palettes of any material is of great interest in chromism-dependent applications.

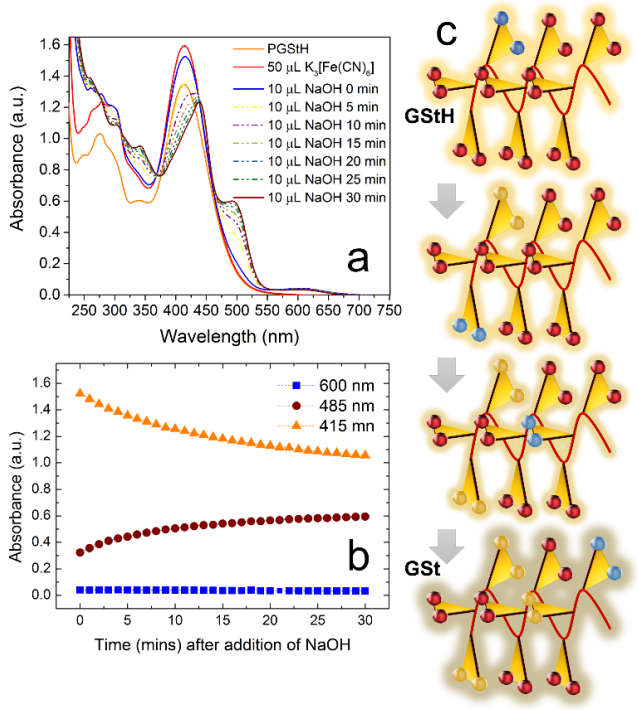

Figure 8. (a) Changes in the UV-Vis absorption profile of GStH (3 mL, 0.1 mM in 1:9 THF-H_2O mixture) upon titration against NaOH (0.1 g mL^{-1}). The emergence of the new peak at 600 nm is due to formation of GStB, which visually changes the color of the solution to dark blue (inset). (b) Reaction of the generate GStB with the gradual addition of $K_3[Fe(CN)_6]$ (10 mM) shows the formation of a new distinct peak at 485 nm. However, the maximum intensity of this peak is observed at the middle of the titration, which indicates that the formed species in unstable in presence of NaOH (aq). (c) The unstable nature of GSt in NaOH (aq) is demonstrated. Addition of excess $K_3[Fe(CN)_6]$ at a single time results in nearly 90% conversion to the radical species; however, a gradual decomposition of this radical species subsequently follows. The inset picture shows the immediate disappearance of the blue color of GStB upon addition of $K_3[Fe(CN)_6]$.

<u>Thrust 2: Controlling Charge Transfer at Metal-Organic Interfaces with Radical Polymers and Increasing the Electrical Conductivity of Radical Polymers</u>

The second specific aim of this project was to control the energy and charge landscape at the interface of metallic contacts and organic semiconductors using radical polymers, as this junction is known to impact the performance of myriad organic electronic devices. In our first efforts, we used the standard testbed geometry of the OFET to evaluate our ability to accomplish

this objective. This is because one of the most implemented techniques with respect to modifying the metal-semiconductor interface is the insertion of a thin layer between the metal and semiconductor layers. The specific material of interest can range from self-assembled monolayers (SAMs) of electrically-insulating species to electrically-conductive conjugated polymers [*e.g.,* poly(3,4-ethylene dioxythiophene) doped with poly(styrene sulfonate) (PEDOT:PSS)]. In all of these instances, however, the organic interlayer has always consisted of molecules with closed-shell designs. We altered this archetype through the introduction of an open-shell molecule and radical polymer, poly(2,2,6,6-tetramethylpiperidine-1-oxyl methacrylate) (PTMA), as a thin interfacial modifying layer. Specifically, the preference of PTMA to be oxidized to the cation state (in a manner analogous to that typically associated with p-type transport in conjugated organic electronic systems) and its Singularly Occupied Molecular Orbital (SOMO) energy transport level of ~5.2 eV removed from vacuum make it compatible as a hole charge carrier pathway with many well-studied small molecule and macromolecular conjugated organic semiconducting materials. These molecular advantages, combined with the critical need to tune the interfacial properties in organic field-effect transistors, provide one of the great potentials for radical polymers to impact the thin film transistor design paradigm. In our devices, a thin film of PTMA was inserted between the bottom contact gold source and drain electrodes and the thermally-evaporated pentacene semiconducting active layer. Importantly, the PTMA thin film was deposited in a high-throughput manner, with high spatial resolution, using an advanced inkjet printing technique. In this way, the PTMA interlayer was deposited only between the gold electrodes and the pentacene semiconductor (i.e., PTMA was not present in the active OFET channel as shown in Figure 9).

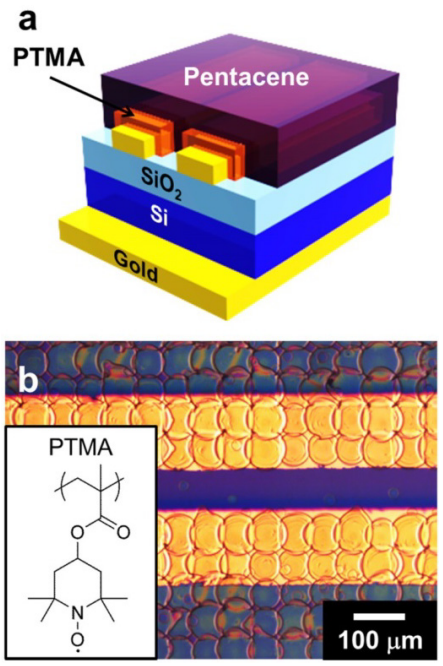

Figure 9. (a) Schematic depiction of the pentacene-based OFET with a PTMA interlayer between the metal contact and the organic semiconductor. (b) Optical microscope image of inkjet-printed PTMA droplets on the gold source and drain electrodes. Note that the resolution of the inkjet printing process allows for the deposition of the PTMA only above the gold contacts and not in the channel of the OFET (i.e., the SiO_2 region between two electrodes). The chemical structure of PTMA is inset.

The inclusion of the PTMA layer significantly improved the performance of the pentacene-based OFETs. Figure 10 shows the output curves [i.e., the drain current (I_D) versus the drain voltage (V_D)] and the transfer curves [i.e., the drain current (I_D) versus the gate voltage (V_G)] of an OFET without a PTMA interlayer and another OFET with a PTMA interlayer (with a thickness of ~8 nm) that was deposited from a 3 mg mL^{-1} toluene solution. In fact, the PTMA interlayer drastically enhanced the charge carrier (hole) mobility and ON/OFF current ratio of the pentacene-based OFET devices. The pentacene OFETs fabricated without the PTMA layer have an average hole mobility (μ_{avg}) of 5.0×10^{-3} cm^2 V^{-1} s^{-1} and an ON/OFF current ratio (I_{ON}/I_{OFF}) of ~10^2. On the other hand, the insertion of the PTMA layer improved the OFET mobility by an order of

magnitude (6.3×10^{-2} cm^2 V^{-1} s^{-1}) and the ON/OFF performance by three orders of magnitude (*i.e.,* to ~10^5). By surmounting this limitation, compared to the unmodified gold (i.e., 0 nm of PTMA) OFET, the OFET with the optimized PTMA interlayer exhibited slightly higher ON current values and drastically lower OFF current values, as shown in Figure 10. Particularly, the OFF current suppression occurs due to an improvement of interfacial transport between gold and pentacene in bottom-contact configuration. As such, the optimized PTMA interlayer successfully facilitates the charge injection between gold and pentacene, as well as the increased hole mobility at the channel region related to higher ON current. Currently, we are designing and synthesizing radical polymer species with SOMO transport levels that are nearer to vacuum than that of PTMA. We anticipate that these macromolecules will serve well in the same function but for n-type OFETs (as opposed to the currently-reported p-type OFETs) upon the use of the appropriate polymer semiconductor and metal contacts. In this way, we aim to demonstrate the universality of the approach to using radical polymers as interfacial modifying layers in a number of different OFET systems.

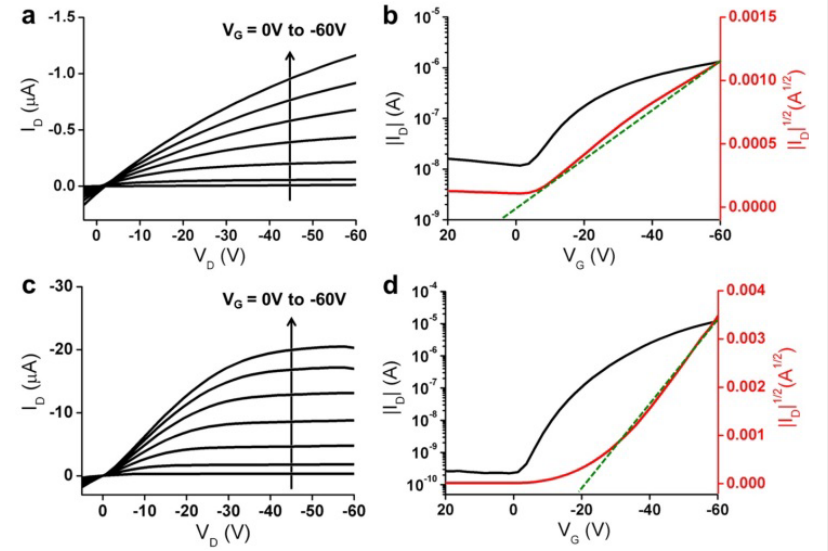

Figure 10. Representative (a) output characteristics (I_D-V_D) and (b) transfer characteristics (I_D-V_G) of pentacene-based OFET devices without a PTMA interlayer. Representative (c) output and (d) transfer characteristics of pentacene-based OFET devices with ~8 nm of PTMA deposited between the organic semiconductor and the gold electrodes. The transfer curves shown in parts (b) and (d) were acquired at a gate voltage of V_G = –60 V.

Moreover, we expanded in order to incorporate PTMA as a charge extraction layer in a perovskite solar cell. This collaborative work, in conjunction with photophysics and perovskite solar cell expert Professor Xiong Gong (University of Akron), was the first demonstration of a radical polymer being used in a perovskite solar cell. In particular, we reported on high-performance perovskite solar cells (PSCs) through the utilization of a crosslinkable radical copolymer, poly(2,2,6,6-tetramethylpiperidinyloxy-4-yl methacrylate)-*co*-(4-benzoylphenyl methacrylate) (PTMA-BP) with a low-lying transport energy level of –5.1 eV (relative to vacuum) to engineer the surface of the PEDOT:PSS hole-transporting layer (HTL). The benzoylphenyl methacrylate portion of PTMA-BP was crosslinked under ultraviolet (UV) light in order to provide a robust surface on which to cast the perovskite (methylammonium lead triiodide, $CH_3NH_3PbI_3$) precursor solution while the PTMA moieties within the copolymer served as the means by which to transport charge from the photoactive layer to the PEDOT:PSS HTL. The current density versus voltage (J-V) characteristics of PSCs as a function of different thicknesses of the PTMA-BP thin film layers processed from precursor solutions with different concentration indicated that the enhancement on open-circuit voltage (V_{OC}) comes from the combination of better band alignment with the photoactive layer as well as a surface passivation effect (Figure 11).

Also, the addition of the PTMA-BP interlayer reduced the reverse dark current of the PSCs, consistent with the observed increase in V_{OC}. Through contact angle measurements of the HELs and scanning electron microscope (SEM) imaging of the $CH_3NH_3PbI_3$ thin film formed on the chemically-distinct modifying layers, the chemically-robust and relatively non-wetting surface of PEDOT:PSS/PTMA-BP HTL improved the crystallization of perovskite materials and allowed for the creation of larger and more uniform semiconducting crystalline domains (Figure 12); in turn, this gave rise to improved device performance as described above. In addition, the study on the light intensity dependence on J_{SC} and V_{OC} suggested that there was suppressed surface recombination due to the introduction of the PTMA-BP layer. Furthermore, the investigation of PSCs by transient photocurrent (TPC) measurements reveals that the charge extraction on the interface between the HEL and $CH_3NH_3PbI_3$ active layer was dramatically promoted when we introduced a PTMA-BP thin layer on the top of the PEDOT:PSS HEL. As a result, the short-circuit current (J_{SC}), V_{OC}, and fill factor (FF) were all improved through the inclusion of a properly-tuned PTMA-BP layer, which provided an over 15% enhancement on power conversion efficiency (PCE). Thus, this collaborative work was important for three key reasons. First, it established a relationship between two laboratories within the Organic Materials Chemistry program that have complementary skill sets. In this way, both groups were able to maximize their productivity while also bringing new avenues of work to their research portfolios. Second, this effort demonstrated the robust nature of radical polymer interlayers with respect to different device geometries and semiconducting active layers. Therefore, this work highlights the idea that radical polymers really are a platform material for solid-state electronic device applications. Third, the introduction of the UV-crosslinkable sites within the radical polymer backbone demonstrated the ability of our group to synthesize materials that can be printed onto myriad substrates and then serve as substrates themselves.

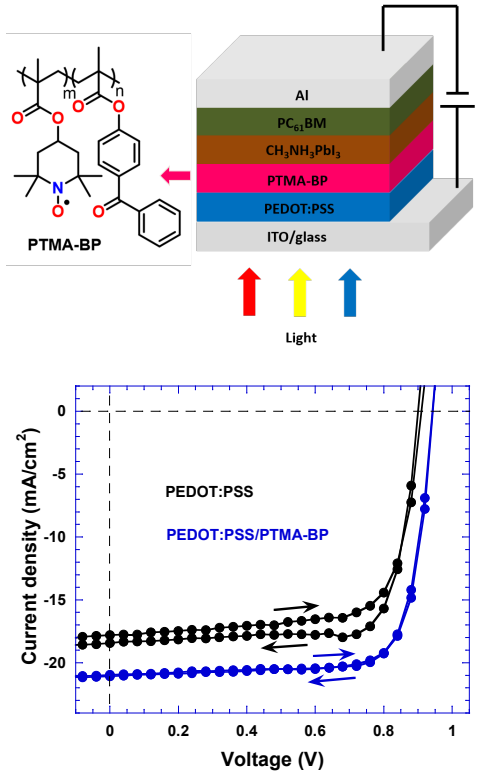

Figure 11. (Top) Chemical structure of PTMA-BP and the device structure of the PSC used in this study. (Bottom) Representative J-V curve for two devices: one that includes the PTMA-BP interlayer and one that does not include the radical polymer. Clearly, the radical polymer interlayer improves performance.

In fact, we utilized this crosslinkable moiety in yet another organic electronic application that was based on an ion-penetration mechanism. Specifically, a highly-transparent crosslinkable thin film made of the radical polymer PTMA-co-BP was developed as the ion storage layer in electrochromic devices (ECDs). After photo-crosslinking, the dissolution of PTMA-co-BP in electrolytes was mitigated, which resulted in an enhanced electrochemical stability compared with the homopolymer PTMA thin film. Moreover, the redox capacity of PTMA-co-BP increased

because of the formation of a crosslinked network. By matching the redox capacity of the PTMA-co-BP thin film and bis(alkoxy)-substituted poly(propylenedioxythiophene), the ECD achieved an optical contrast of 72% in a small potential window of 2.55 V (i.e., switching between +1.2 and −1.35 V), and it was cycled up to 1,800 cycles. The ECD showed an excellent optical memory as its transmittance decayed by less than 3% in both the colored and bleached states while operating for over 30 min under open-circuit conditions. Use of crosslinkable radical polymers as the transparent ion storage layer opens up a new venue for the fabrication of transmissive-mode organic ECDs.

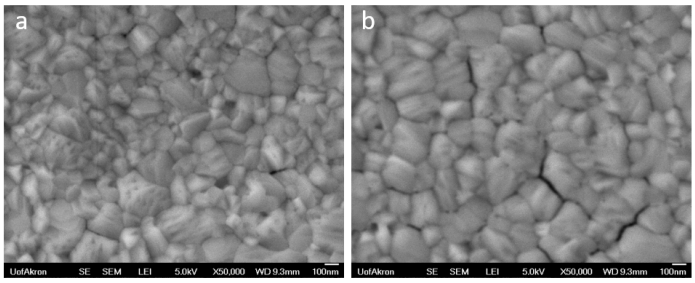

Figure 12. Scanning electron microscopy (SEM) images of perovskite thin films grown on (a) PEDOT:PSS and (b) PTMA-BP radical polymer substrates. The increased grain size of the perovskite layer grown on PTMA-BP is one of the many reasons why devices with the radical polymer interlayer outperformed the standard device structure with respect to the final PCE obtained. The scale bar represents 100 nm.

In addition to manipulating the polymer structure through copolymerization with crosslinkable units, it also is critical to alter the absolute electrical conductivity of the radical polymers in these systems in order to minimize contact resistance at the organic-metal interface. As such, we have placed significant efforts in increasing the electrical conductivity of non-conjugated radical polymers. In the first of these efforts, we began doping radical polymer systems with redox-active salts, in order to increase the electrical conductivity of the materials relative to the pristine radical polymers. Specifically, we combined a model radical polymer, PTMA, with a small molecule redox-active salt, 4-acetamido-2,2,6,6-tetramethyl-1-oxopiperidinium tetrafluoroborate (TEMPOnium), in order to elucidate the effect of molecular doping on this emerging class of functional macromolecular thin films. Note that the TEMPOnium salt was specifically selected because the cation in the salt has a very similar molecular architecture to that of an oxidized repeat unit of the PTMA polymer. Importantly, we demonstrated that the addition of the TEMPOnium salt simultaneously alters the electrochemical environment of the thin film without quenching the number of open-shell sites present in the PTMA-based composite thin film. This environmental alteration changes the chemical signature of the PTMA thin films in a manner that modifies the electrical conductivity of the radical polymer-based composites. Therefore, these data established an underlying mechanism of doping in electronically-active radical polymers, and they provided a template by which to guide the design of next-generation radical polymer composites.

Importantly, the addition of the small molecule TEMPOnium to the PTMA thin film increased the conductivity of the thin film by a factor of 5 at the optimized loading condition (i.e., 8% TEMPOnium), as shown in Figure 13. This increase in electrical conductivity was a result of the additional cation sites that can participate in the charge transport redox reaction, as well as the contributions that existed from the counter anion stabilizing these cation sites. The inclusion of these electron-deficient nitrogen cation sites increased the overall hole density within the system, thereby increasing the charge transport ability of the radical polymer. As each cation salt was added, the ratio of radical to cation species was changed. In turn, this promoted the charge transfer reactions throughout the system due to the increased presence of an electron deficient species

acting as acceptor sites for the radical sites. Furthermore, by adding the small molecule salt, the intermolecular packing within the film changed. It is possible that this decreased the site-to-site distance for a charge hopping event, on average, and this has been computationally-predicted to improve the charge transport ability of PTMA. From a macroscopic perspective, this allowed for more charges to travel across the thin film from one electrode to the other without being localized to a redox site that is isolated from other redox sites for a significant period of time (i.e., a deep trap site). Note that all of the samples were transiently biased at a sweep rate of 3 V s^{-1} to ensure that the sweep rate was fast enough to make ionic contributions negligible, as has been demonstrated previously.

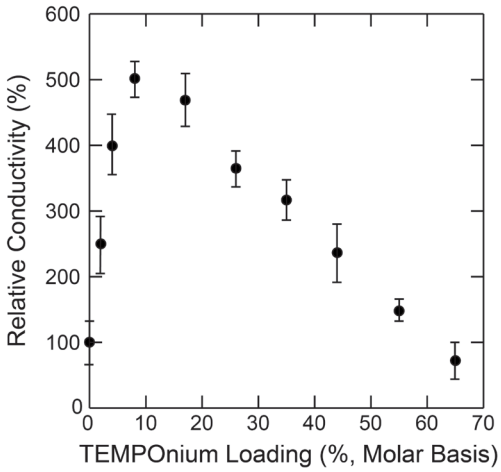

Figure 13. The relative conductivity of PTMA thin films as a function of TEMPOnium loading. The geometry used for the conductivity experiments was one that used PEDOT:PSS coated onto ITO and Au as the two contacts of the thin film as the work functions of these two materials have useful electronic alignment with the transport level of PTMA (i.e., an ohmic-like contact is made). The maximum in electrical conductivity occurs at a TEMPOnium loading of 8% (on a molar basis) to produce a material that has a 5-fold increase in electrical conductivity relative to pristine PTMA.

In order to confirm that the increase in electrical conductivity was due to interaction between the TEMPOnium and PTMA repeat units specifically, control experiments were performed. The use of TEMPOnium as a dopant for the poor conducting closed-shell precursor to PTMA, PTMPM, showed no enhanced electronic performance. The (relatively low) conductivity of the TEMPOnium loaded PTMPM was marginally different (1.5-fold increase) relative to the pristine PTMPM film. This was significantly lower than the 5-fold increase observed for the PTMA and TEMPOnium blend. Furthermore, the absolute conductivity of this blend was much lower than that of the radical polymer-based system. Moreover, the use of a different salt that lacked the TEMPOnium functionality, tetrabutylammonium tetrafluoroborate, as a dopant for PTMA also showed no trend in electronic performance. In fact, the conductivity of these two systems (tetrafluoroborate salt doped PTMA and pristine PTMA) differed by less than 5%. This indicated that the increase in electrical conductivity when using TEMPOnium as a dopant is due to the redox interaction between the TEMPOnium and PTMA. As such, we were able to demonstrate how the interactions between the radical polymer and the small molecule dopant needed to be balanced in order to achieve the desired outcome. While this increase was important, it also lead to (arguably) the most significant breakthrough during the period of performance. That is, we were able to increase the electrical conductivity of a targeted radical polymer be many orders of magnitude through appropriate molecular design.

We attempted this effort despite the fact that our group has set the current record for the highest solid-state electrical conductivity; however, this was reported at ~10^{-4} S cm^{-1}, and this value is still rather low. Thus, many radical polymer-based interlayers have to be extremely thin (~10 – 30 nm). Of course, this limits the wide-scale feasibility of such materials in many practical applications. Because of this fact, we set our sights on increasing the solid-state electrical

conductivity of radical polymers through appropriate molecular design. While offerings have arisen that suggest that the ~10^{-4} S cm^{-1} value could perhaps be the fundamental limit of these materials due to their lack of conjugation and their amorphous nature, there is no stringent limitation to the ultimate electrical conductivity of these materials as the redox reactions that allow for charge exchange between the pendant groups are rapid. Here, we addressed this issue in a direct manner. A critical design parameter in the syntheses of high electrical conductivity radical polymers is to create materials with a high density of radical sites, as increasing the concentration of radical sites along the radical polymer backbone has been shown to increase the conductivity of radical polymers in an exponential manner. Therefore, polymerizing a monomer that contained an open-shell site directly was preferred relative to polymerizing a closed-shell monomer and subsequently converting this closed-shell species to an open-shell species (i.e., through post-polymerization functionalization). This is because we demonstrated that (during previous AFOSR support) the post-polymerization functionalization reaction rarely results in complete pendant group conversion from a closed-shell site to an open-shell site, and it usually leads to undesired byproduct pendant group chemistries as well. Fortunately, a nitroxide functionality could be added to a common monomer by reacting epichlorohydrin with TEMPO in the presence of a base (Figure 14), and this small molecule product was purified to a high degree in order to ensure a single pendant radical group per monomer unit. Then, this monomer was a reactant in a ring-opening polymerization reaction, where potassium *tert*-butoxide served as the initiator, in order to generate the well-defined PTEO radical polymer with a number-average molecular weight of 2.4 kg mol^{-1}. Because this macromolecule was formed through a polymerization scheme that did not include a radical intermediate, the high density of radical sites that were present in the monomer were also present in the fully-formed PTEO.

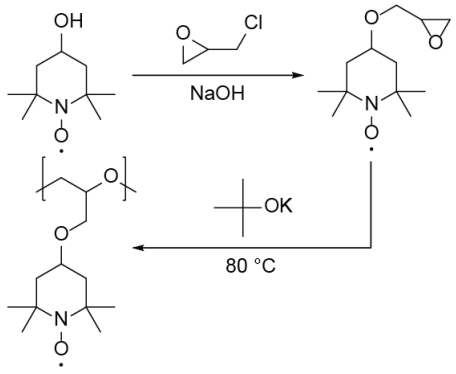

Figure 14. The monomer synthesis and ring-opening polymerization-based synthetic scheme utilized to generate the PTEO radical polymer.

The second design metric for a radical polymer to have a high electrical conductivity as a thin solid film is that the macromolecule should exhibit a solid-like to liquid-like transition at relatively low temperatures. That is, there should be a large window between the flow transition temperature of the open-shell macromolecule and the degradation temperature of the radical pendant groups. Of course, this type of design can be tailored with radical polymers as the backbone of the macromolecule dominates the mechanical and thermal properties observed for the polymer while the decoupled pendant groups dictate the electrochemical nature of the material. Again, this is in contrast to a number of common conjugated polymers where the macromolecular backbone dictates many of the final performance metrics and pendant groups are typically added solely to increase the solubility of the organic electronic material in organic solvents. In terms of generating a low glass transition temperature radical polymer, PTEO served as a useful material. This design was implemented because the simplest closed-shell analog of PTEO, poly(ethylene oxide) (PEO), was known to have a low glass transition temperature despite the fact that PEO was a solid at room temperature due to the fact that the melting temperature of the material is ~50 °C.

However, the bulky nitroxide-containing substituent of the PTEO prevented crystallization of the polymer chains. Moreover, due to the polar nature of the nitroxide moiety, the glass transition temperature (T_g) was raised, relative to PEO, to T_g ~15 °C, as estimated from differential scanning calorimetry (DSC) data. This near-room temperature glass transition temperature was an experimentally convenient temperature by which to probe how the electronic properties of the material were impacted as a function of temperature above and below T_g in this non-conjugated, amorphous polymer system. That is, due to their glassy nature and the fact that they are usually cast from high volatility organic inks (as they are readily soluble in myriad organic solvents), the coating of radical polymer thin films for solid-state organic electronic applications has typically led to materials with packing structures far-removed from equilibrium, which resulted in relatively low electrical conductivity values for the thin films. While increasing the number of open-shell sites along the macromolecular chain has allowed this value to increase by approximately 10-fold, closing the large conductivity gap between open-shell macromolecules and traditionally-doped conjugated polymers required a fundamental change in the molecular design approach. That is, the relatively rapid redox kinetics associated with nitroxide radicals in electrolyte-supported systems was well-known. In the solid state, however, the radical site proximity has never been intimate enough to take advantage of this key aspect.

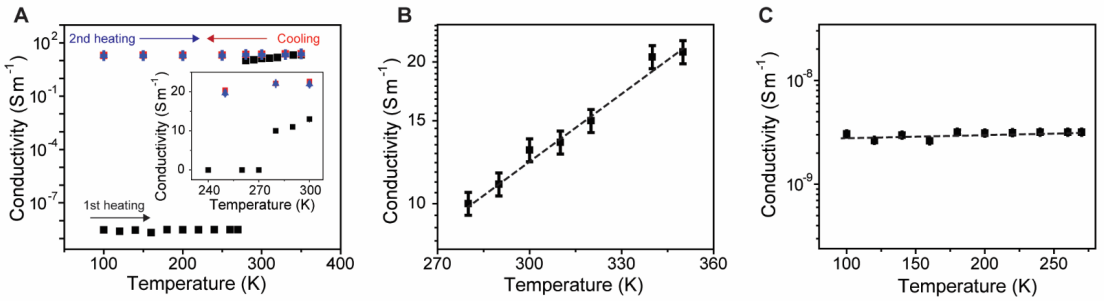

Figure 15. PTEO conducts charge after annealing has occurred. (a) Electrical conductivity as a function of temperature for PTEO in a 0.5 μm channel. Real-time annealing of the thin film allowed for local order to appear within the film such that the electrical conductivity was altered by ten decades. (b) Above the glass transition temperature, there is thermally-activated transport while (c) below the glass transition temperature the electrical conductivity is temperature independent. The data points represent the average value measured for 4 different PTEO films, and the error bars represent the standard deviation from this average. If no error bars are present, the error is within the size of the point.

We monitored this transition for PTEO from the low charge transport regime (~10^{-9} S m^{-1}) to the high charge transport regime (~10 S m^{-1}) in real time as the material crossed from the as-spin-coated glassy state (i.e., the thin film was cast at ~20 °C) into liquid-like molten state (Figure 15a). In order to evaluate charge transport in this quenched state, the films were transferred to an inert atmosphere vacuum probe station and held at a temperature of 100 K. Heating of the sample occurred inside of the inert atmosphere vacuum probe station in order to capture the charge transport ability at low temperatures prior to bringing the PTEO thin films near T_g, so the changes in conductivity appear to be caused by changes in the nanoscale structure as opposed to changes in chemical oxidation. In these experiments, the sample was allowed to reach the desired temperature and held at that temperature for 30 minutes prior to collecting the electrical data. Then, the temperature of the sample was moved to the next temperature. Moreover, in a separate experiment, replicate devices were annealed at 80 °C for 2 hours in inert atmosphere conditions but without evaluating their low-temperature electrical properties (i.e., without the "1st Heating"

scan in Figure 15a), and the conductivity of thin films processed in this manner began and remained at ~10 S m^{-1} (i.e., in the same manner seen for the "2nd Heating" scan of Figure 15a), indicating that ordering was occurring though thermal annealing. Once local order was created within the melt, it was retained as the thin film was cooled back into the glassy state, and this enabled rapid charge transport at room temperature both for cooling (red squares) and heating (blue triangles) of the thin film. Above T_g, thin films displayed thermally-activated transport with an activation energy of ~90 meV (Figure 15b), consistent with the increased molecular motion. Moreover, as has been observed with other radical polymers, the transport was independent of temperature below T_g (Figure 15c).

Moreover, this annealing procedure was performed prior to electrical characterization, and the conductivity of the thin film began (and remained) at ~0.1 S cm^{-1}, indicating that ordering was occurring though thermal annealing in this PTEO system. Once this local order was found within the melt, it was retained as the thin film was cooled back into the glassy state. That is, after initial thermal annealing of the radical polymer thin film, which was not possible for many radical polymer species due to thermal degradation concerns, this local structure of the glass was connected in such a way that rapid charge transport occurred. This was the case both for cooling (red squares) and heating (blue triangles) of the thin film. This speaks to the fact that the phenomenon observed here may not be unique and that many non-conjugated, redox-active polymers could possibly undergo this type of behavior. However, this type of electrical conductivity has not been observed in radical polymers due to the inability to thermally-anneal these materials well. Thus, this avenue of study could prove promising with respect to design considerations of next-generation amorphous radical polymers. Additionally, the non-conjugated nature of the radical polymers was also quite apparent in these samples due to the weak absorption profiles of the material both in solution and as thin films. That is, the solution absorption spectrum showed the oft-observed signal for nitroxide-based radical polymers, and this highlighted the presence of the optically-active open-shell moieties along the PTEO chains. However, the ~1 μm-thick PTEO film showed only minimal absorption in the visible spectrum (i.e., ≥ 98% transmission at wavelengths of $\lambda \leq 500$ nm and 100% transmission at longer wavelengths). The combination of these two key results demonstrated that properly-designed and appropriately-processed radical polymers have true potential in next-generation transparent conductor applications.

As mentioned previously, above the glass transition temperature of the PTEO, the thin film displayed thermally-activated transport with an activation energy of ~90 meV. This is consistent with the idea that there was increased molecular motion within the liquid-like material at these elevated temperatures, and thus, there was an increased likelihood of radical-radical interactions from open-shell sites that were not necessarily in electronic communication when the polymer was a glass. As has been shown numerous times by our group previously for radical polymer systems, the transport was independent of temperature across a wide range of temperatures when the thin film was below T_g. Thus, the rate-limiting step in charge transport in these materials is not the actual electron exchange reactions. This is consistent with previous computational efforts and the rapid reaction kinetics associated with the redox behavior of radical systems. Moreover, and unlike in conjugated polymer systems, the charge transfer site is heavily localized on the nitroxide group. Thus, any changes in structure along a polymer chain caused by crystalline domains, added or disrupted conjugation, or alterations to the polymer configuration (e.g., kinks along the chains) did not impact the charge transport abilities of radical polymers. Instead, the ability to form regions

where there were significant interactions between radical groups was what dominated the observed electrical conductivity. Previously, this interaction distance has been computationally estimated to be ~0.5 nm, and if radical sites located within a single domain were within this spacing of one another, transport should happen in a rapid manner.

Unlike many conjugated polymer systems, the lack of crystallinity in these amorphous conductors, made it difficult to experimentally-determine the exact length scale at which the localized interactions occurred. While solid-state EPR data showed significantly more radical-radical interactions (i.e., through the removal of hyperfine splitting and the emergence of a single Lorentzian peak) in the solid-state versus in solution (data not shown), this technique was not able to specifically identify the length scale of these interactions. However, we were able to estimate the size of these communicating, high charge transport domains through the introduction of varying channel lengths between the two gold electrodes.

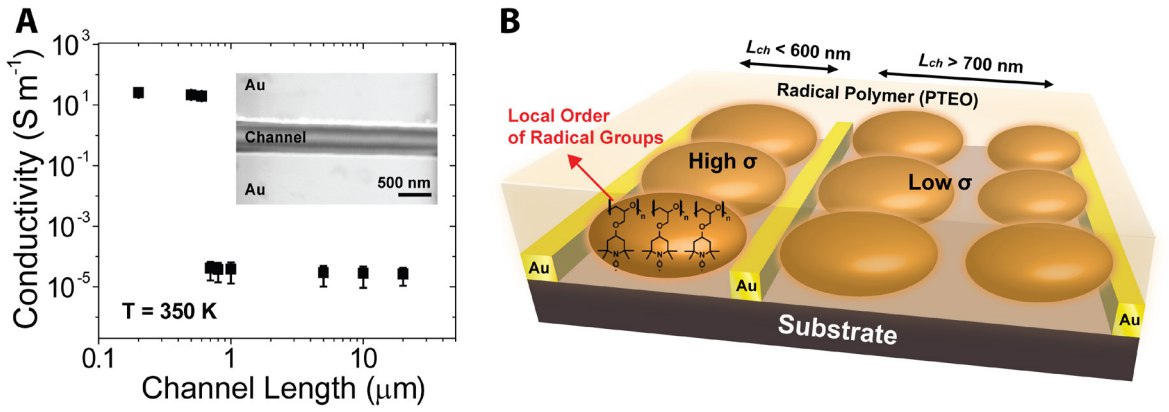

Figure 16. The charge transport behavior of radical polymers was dictated by domains within the glassy thin films that contained local order and allowed for charges to pass through the rapid redox reactions between the open-shell moieties. (a) The electrical conductivity at T = 350 K as a function of channel length shows that these localized domains were less than or equal to 600 nm in size. The data points represent the average of the measurements conducted on 4 different devices of that channel length, and the error bars represent one standard deviation from this average. If no error bar is shown, the error is within the size of the point of datum. The inset shows a scanning electron microscopy (SEM) image of a typical channel used in these studies showing the clear spacing between the gold electrode contacts prior to film deposition. (b) Cartoon depiction of the fast and slow domains within the amorphous radical polymer thin film. The hard orange spheres represent domains within the glass that allow for fast charge transport while the lightly shaded region highlights the low charge transport regimes that surround the islands of high charge transport in longer channel devices.

In particular, Figure 16a shows the electrical conductivity of the PTEO thin films as a function of channel length. At longer channel lengths, the electrical conductivity of the thin films reached a value of ~10^{-6} S cm^{-1}. This was in agreement with many previous reports on the electrical conductivity of radical polymers and spoke to a film that contained a number of regions of low transport being present between the metal contacts. However, as the channel length was decreased to 0.6 μm or less, the conductivity reached ~0.2 S cm^{-1}. We note that multiple control samples consisting of a bare channel (i.e., with only the insulating silicon dioxide substrate present) and a channel that contained a known electronically-inactive polymer, polystyrene (PS), were fabricated and tested to ensure that the conductivity values obtained in the shorter channels were not due to the fabrication or processing conditions used for the organic electronic devices. Thus, these data pointed to the idea that the local order within the glass had a domain spacing of ~600 nm (Figure

16b) and that these regions were responsible for the rapid transport of charge due to solid-state redox reactions. This is not unlike many emerging high mobility conjugated polymers that show no or little scattering in wide-angle x-ray scattering (WAXS) experiments. However, radical polymers lack a conjugated backbone or tie chain pathway for charge transport between their aggregate domains and this means that, if the high charge transport domains do not bridge across the electrodes, the transport is severely limited by the low charge transport domains of the redox-active macromolecules. On the other hand, the idea of polymer glasses having local order is emerging in many fields of materials science, and the data presented here support the concept of having sub-micron regions (i.e., grains) of intermediate order that are surrounded by regions of complete disorder with respect to the ability of one radical site to efficiently communicate with another open-shell site within the glassy thin film. While this concept has not been addressed to a large degree in the realm of conducting polymers, the potential use of these redox-active moieties to probe the underlying phenomena associated with the glassy state could provide a key handle (i.e., electrical conductivity) in deciphering the true nature of the glass, one of the most intriguing questions in solid-state physics today.

In addition to having high electrical conductivity values, we note that these undoped radical polymer thin films maintained their high electrical conductivity over multiple months when they were exposed to ambient conditions; this is in agreement with previous reports of the relative stability of the nitroxide radical when it was incorporated into a macromolecular architecture. Moreover, this demonstrated another critical difference between redox-active radical polymers and traditional conjugated organic electronic materials, which can be sensitive to ambient conditions. When combined with their completely amorphous nature and temperature-independent transport characteristics, it is clear that radical polymers offer a previously-unexamined opportunity outside of the realms typically considered for closed-shell macromolecular conductors. As such, we have taken the first step in demonstrating the true potential of radical polymers as optically-transparent, charge-neutral conductors with electrical conductivity values of ~20 S m^{-1}. While open questions still remain regarding the exact structure and chemical nature of the high charge transport regimes that allow for these high electrical conductivity values, the clear presence of these regimes offers a distinct design handle by which to molecularly engineer future generations of this type of open-shell macromolecule and are the first data to introduce the concept of charge-neutral conducting polymer glasses. Thus, we believe that we have positioned our team to be the world leader in understanding the transport in these materials, and in turn, this will allow us to synthesize materials systems that will afford for a clear path forward for transparent, flexible, and stretchable electronic devices.

<u>Thrust 3: Controlling the Thermoelectric Properties of Conjugated Polymers using Open-Shell Dopants</u>

In addition to controlling the flow of charge and energy at organic-organic and inorganic-organic junctions in organic electronics, this work aimed to tackle the flow of charge and heat in thermoelectric (TE) materials as well. Based on preliminary results from our previous work, we hypothesized that radical additives would have a significant impact in generating higher-performing organic electronic thermoelectric modules. While most of the highest-performing thermoelectric materials to date incorporate rare earth metals (e.g., tellurium), the scarcity of their components coupled with costly high-temperature processing conditions (and their potential

toxicity) has driven interest in earth-abundant alternatives for low-temperature thermoelectric materials. Furthermore, the low phonon mean free path, which is typically associated with a low thermal conductivity (κ ~0.2 W m^{-1} K^{-1}), associated with organic materials makes them an attractive alternative to traditional inorganic materials. Consequently, the most significant term in the figure of merit equation, from a polymer thermoelectric optimization standpoint, is that of $S^2\sigma$ (i.e., the power factor). However, optimization of the power factor is often a non-trivial goal due to the classically observed inverse relationship between electrical conductivity and thermopower. Historically in organic electronic systems, the electrical conductivity of hole-transporting (p-type) polymeric materials is enhanced through oxidation of polymer chains; conversely, the resulting shift in the Fermi energy reduces the difference between the Fermi energy and the energy level of the average charge carrier, which results in a decrease in the thermopower.

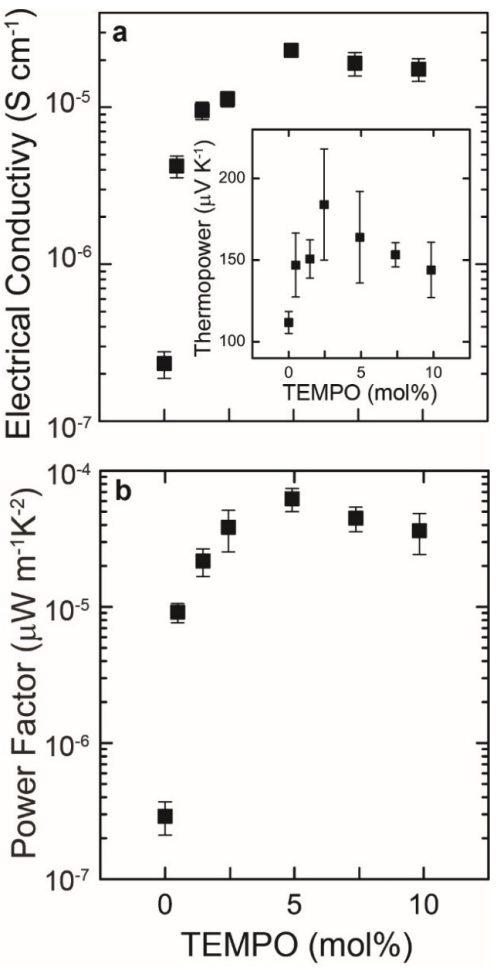

Figure 17. (a) Electrical conductivity and (b) power factor of the TEMPO-containing P3HT composite thin films as a function of TEMPO loading. The thermopower of the composite system as a function of TEMPO loading is inset into panel (a), and this parameter is impacted significantly less than the electrical conductivity as a function of the TEMPO addition.

On the other hand, if the electrical conductivity could be increased without influencing the oxidation state of the polymer itself, it would provide a means by which to circumvent this traditionally observed tradeoff. Therefore, in spite of ongoing efforts to improve power factor values for organic materials, organic thermoelectric power factor values consistently lag behind their inorganic counterparts (e.g., ~56 μW m^{-1} K^{-2} for a high-performing polymer-based composite compared to ~1500 μW$m^{-1}K^{-2}$ for Bi_2Te_3) in low-temperature (i.e., near room temperature) applications due to this tradeoff between increased electrical conductivity and decreased thermopower. Thus, establishing alternative mechanisms to enhance this critical power factor value is vital for the long term interest of polymer thermoelectric materials, and we have begun address this objective here by utilizing an oft-studied hole-transporting semiconducting polymer. While there are several molecular architectures capable of transporting charge via resonance delocalization of π-electrons across a polymer backbone, the well-studied nature of polythiophene-based macromolecules allow them to be a useful testbed system for the introduction of new doping strategies. Furthermore, the charge neutral (i.e., undoped) nature of regioregular poly(3-hexylthiophene) (P3HT) allows for the straightforward analysis of the impact of radical species on the oxidation state of the system. Specifically, we evaluated the effect of incorporating open-shell species with different singularly occupied molecular orbital (SOMO) energy levels into regioregular P3HT. The appropriate

selection of a radical species with a well-tailored SOMO energy level alters the electrical conductivity without negatively impacting the thermopower. Thus, we demonstrated an increase in the thermoelectric power factor of the polymer that is independent of a change to the oxidation state of the semiconducting polymer.

For example, the incorporation of TEMPO resulted in an increase in the electrical conductivity of P3HT even at very low loadings of the open-shell small molecule. While the SOMO energy level of TEMPO is farther removed from vacuum than the lowest unoccupied molecular orbital level (LUMO) energy level of P3HT, the nitroxide species is known to be much more stable in the oxidized form relative to the reduced form. As such, it is unlikely that the TEMPO dopant would serve as an electron-accepting group for the P3HT, and, for this reason, it was not anticipated that the TEMPO would alter the oxidation state of the P3HT. Importantly, the ability of radical species to conduct charge in the solid state has been previously established. While the operational mechanism behind this thermoelectric enhancement has not been determined definitively, this type of improved electrical performance has been observed previously for n-type radical dopants in conjugated small molecule and polymer systems. As we have seen in our hands, no spectroscopic absorption changes (e.g., those indicative of charge transfer states) were observed; however, it was postulated that the radical sites act as a means by which to alter the defect level within the conjugated matrix of the materials. Notably, there is a slight increase in the materials thermopower after incorporation of TEMPO into the P3HT thin film (Figure 17). This is consistent with our previous report regarding the polymer blend of poly(3,4-ethylene dioxythiophene) and poly(styrene sulfonate) (PEDOT:PSS) thin films that were doped with TEMPO. That is, the energy level of the average charge carrier is altered due to an energy filtering effect incurred from the energetically-unfavorable position of the TEMPO SOMO level in relation to the highest occupied molecular orbital (HOMO) level of P3HT. In a manner that is unique relative to previous thermopower gains resulting from TEMPO incorporation into a conjugated system, the electrical conductivity does not decrease below the electrical conductivity of the pristine P3HT thin film with increased TEMPO loading into the P3HT matrix. While the reason for this is not known for certain, a potential explanation for this change should involve the disordered regimes of the material, as the crystalline nature of the TEMPO-P3HT films was not altered. Previously, this increase in charge transport was ascribed to the removal of defects within conjugated polymer thin films by radical dopants, and this is a potential reason for the improvement as well here. Alternatively, the difference in how the TEMPO influences the electrical conductivity of P3HT compared to PEDOT:PSS may be attributed to the substantial morphological differences between the two conjugated polymer-based systems. While these data confirm the prominent role of the radical in enhancing electrical conductivity, it is important to confirm that these gains are decoupled from frequently-reported oxidative doping of P3HT, which would result in a deleterious effect on thermopower with increasing electrical conductivity.

Unlike TEMPO (which is known to prefer oxidation to reduction), the galvinoxyl radical is known to accept electrons and be readily reduced. This, in turn, allows the galvinoxyl radical to simultaneously act as an additional redox-active site while also maintaining the ability to oxidize the P3HT. For this reason, incorporation of the galvinoxyl radical into P3HT allows for a radical species that will interact with the P3HT from a different energetic standpoint. While the electrical conductivity enhancement of P3HT upon the addition of the preferentially-reduced galvinoxyl radical is similar to that of P3HT thin films when they are doped with the preferentially-oxidized

TEMPO small molecule radical species, there is less of a trend with respect to the thermopower of the galvinoxyl -P3HT system as a function of galvinoxyl radical loading. That is, the addition of the galvinoxyl radical does not alter the thermopower of the P3HT composite system relative to the pristine P3HT film; this is distinctly different from the marked increase that was observed for the TEMPO-P3HT systems (insert of Figure 18). However, this is not surprising given that TEMPO is a hole-transporting material and has a SOMO energy level that is further removed from vacuum than the HOMO level of P3HT. By selectively transporting higher energy holes, it is possible to increase the difference in the energy level of the average charge carrier, compared to the materials Fermi energy. The galvinoxyl radical, which does not possess either of the characteristics described above for TEMPO, does not impart this type of charge filtering effect to the radical-containing composite thin film.

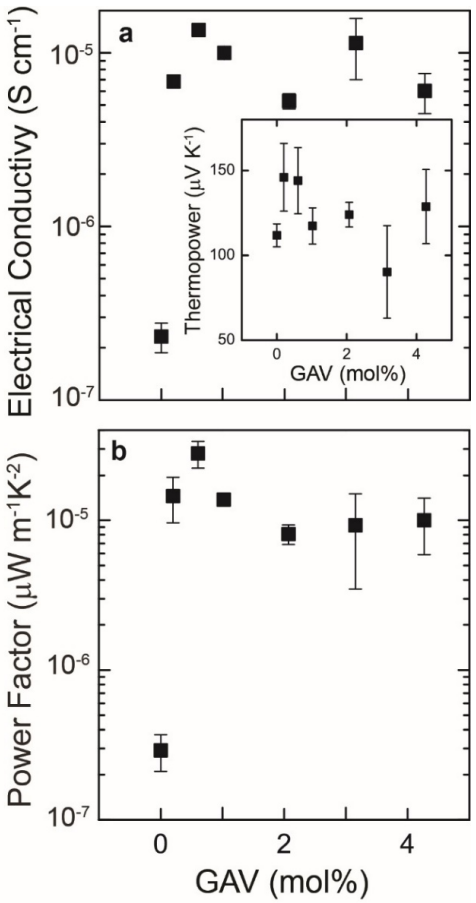

Figure 18. (a) Electrical conductivity and (b) power factor of the galvinoxyl-containing (GAV-containing) P3HT composite thin films as a function of radical loading. The thermopower of the composite system as a function of galvinoxyl radical loading is inset into panel (a).

Therefore, this work demonstrated that open-shell species with a wide range of SOMO energy levels are capable of enhancing the thermoelectric characteristics of π-conjugated polymers. In contrast to many common ionic dopants (e.g., PSS), these electrical conductivity enhancements do not appear to be contingent on a change in the oxidation state of the polymer chains, and thereby offer a possible way to break the traditionally observed inverse relationship between electrical conductivity and thermopower in organic systems. Here, we have demonstrated the ability to elicit a >100-fold increase in electrical conductivity through the application of radical containing materials as molecular dopants. Furthermore, in the case of TEMPO-P3HT, this increase in electrical conductivity occurs without any indication of oxidation of the P3HT chains within the thermoelectric thin films. Thus, this work is the first demonstration of utilizing myriad open-shell materials to transform a classic semiconducting polymer into a promising thermoelectric material. Moreover, this conjugated polymer-radical design motif appears to be general in nature, and, as such, stands to potentially open a new archetype in the design of organic thermoelectric systems.

In fact, we shifted to a conjugated polymer with a lower bandgap than that of P3HT in order to highlight the broad response of conjugated polymers to radical dopants. This was because conjugated polymers (CPs) with narrow band gaps have important properties, such as intrinsic electrical conductivity and open-shell character; however, design rules that favor these properties remain nascent owing to the complex interrelation between electronic properties and

conformational disorder in CP systems. This motivated our design of a narrow band gap copolymer structure comprised of a 4,4-dihexadecyl-4*H*-cyclopenta[2,1-*b*:3,4-*b'*]dithiophene (CPDT) donor and a strong, proquinoidal thiadiazoloquinoxaline (TQ) acceptor (CPDT-*alt*-TQ, or PCQ). This macromolecular architecture was synthesized because fused thiophene donors, such as CPDT, and highly electronegative acceptors, such as TQ, lead to reduced frontier orbital energy separation, enhanced solid-state interactions, and facilitate π-electron delocalization in weakly crystalline systems. Charge transport is generally more efficient in materials with largely delocalized electronic structures, strong electronic interactions between the building blocks, and improved structural and electronic order. General design guidelines for open-shell character further rely on aromatization of embedded quinoidal subunits resulting in stabilization of the singlet diradical (biradicaloid) resonance form. These design parameters, acting synergystically, demonstrate that solution-processable DA copolymers that exhibit intrinsic electrical conductivity and open-shell character can be readily achieved.

Due to the low band gap and biradicaloid nature of the CP, a pristine thin film of PCQ behaved more like a doped semiconductor at room temperature, rather than a neutral undoped organic semiconductor. This was despite the fact that the grazing-incidence wide-angle X-ray scattering (GI-WAXS) profile of a PCQ thin film showed that the material was weakly crystalline even after annealing. That is, there were weak first-order alkyl stacking peaks (100) present at $q \approx 0.24$ Å^{-1} ($d \approx 26.17$ Å) in the in-plane direction and $q \approx 0.25$ Å^{-1} ($d \approx 25.12$ Å) in the out-of-plane direction. The presence of the in-plane stacking peaks (001) at $q \approx 0.52$ Å^{-1} ($d \approx 12.08$ Å) and (002) at $q \approx 1.10$ Å$^{-(}$ ($d \approx 5.71$ Å) were attributed to the chain backbone ordering. The broad hump from 1.2 to 1.6 Å^{-1} was attributed to the scattering from the amorphous regions within the film. The out-of-plane stacking peak (010) presented at 1.65 Å^{-1} gave a π-spacing of 3.81 Å with a face-on π-π stacking pattern. This type of behavior (i.e., high electronic performance in the absence of large degrees of crystallinity) has recently been reported for a number of CPs.

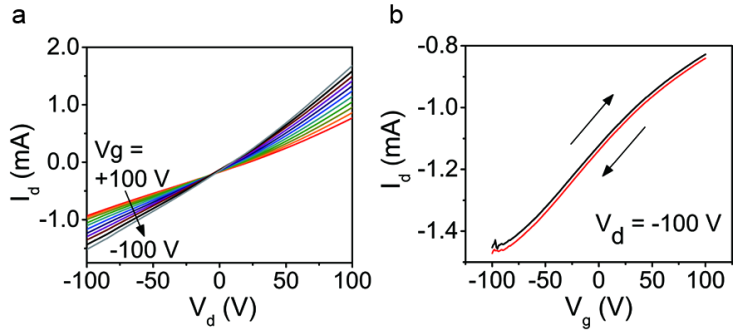

Figure 19. Electronic characteristics of a typical field-effect transistor (L = 100 µm, W = 1 cm) based on PCQ. (a) Output characteristic at varying gate voltages demonstrating the transport behavior of PCQ without achieving saturation from V_g = +100 V to V_g = –100 V and (b) the transfer curve showing that the device does not turn off at any gate voltage value.

In fact, when implemented in a transistor geometry at room temperature, PCQ did not display the ability to reach a saturated state, nor did PCQ show any type of ON current to OFF current ratio (Figure 19). Thus, even in the undoped state, the open-shell macromolecule behaved in a manner that was more akin to what is seen for classic polymer conductors like PEDOT:PSS. That is, the application of the electric field through the gate electrode did not drastically alter the number of free charge carriers available in the PCQ system. Despite this behavior, the mobility of the pristine PCQ was determined from the linear regime of the current-voltage sweeps in a transistor geometry. That is, we analyzed the mobility via a definitive transistor model, according to the following equation.

$$\mu = \frac{g}{V_D C_{OX}} \frac{W}{L}$$

Here, g is the transconductance, L is the channel length, W is the width of the device V_D is the source-drain potential, and C_{OX} is the capacitance of the dielectric layer (300 nm thick silicon dioxide). The mobility achieved by PCQ here was 0.026 $cm^2\ V^{-1}s^{-1}$. Importantly, this point speaks to the idea that the proper design of low band gap conjugated radical polymers can lead to materials that move beyond the standard CP design paradigm. These molecular design features demonstrate that neutral DA CPs can be generated such that they show promising and tunable electrical conductivity values and linear current-voltage characteristics in the absence of intentional dopants. These unique electronic structures serve as a handle by which to modulate the electrical conductivity and the interrelated parameters associated with thermoelectric performance.

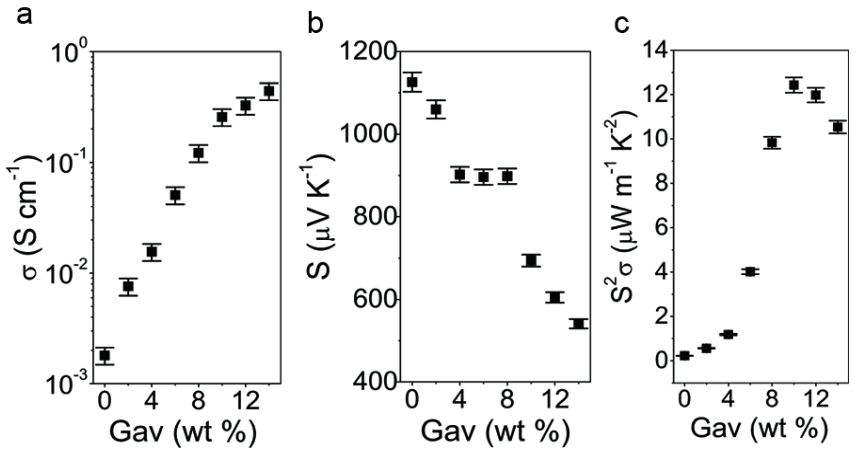

Figure 20. (a) Electrical conductivity, (b) Seebeck coefficient, and (c) power factor of the galvinoxyl radical-containing (Gav-containing) PCQ composite thin films as a function of Gav loading. Each data point represents the average of measurements collected on three measurements, and the error bars represent one standard error from the average.

The electrical conductivity of pristine PCQ is rather large, at a value of 10^{-3} S cm^{-1}, given the undoped nature of the conjugated radical polymer; however, the addition of just 10% (by weight) of galvinoxyl radical to the system increases the electrical conductivity of PCQ by two orders of magnitude to 10^{-1} S cm^{-1}. Previously, small molecules and radicals have been utilized to dope both PEDOT:PSS and poly(3-hexylthiophene) (P3HT). There are two distinct differences between the previous data (*vide supra*) and the current discussion. First, the baseline (i.e., in the absence of dopants) electrical conductivity of P3HT was significantly less than that of PCQ. Thus, the fact that the galvinoxyl radical was able to manipulate the charge carrier density in both systems in a similar manner (and at similar loadings) speaks to the ability of open-shell units to interact synergistically with a myriad of CP backbones. Second, unlike P3HT, the PCQ polymer possessed open-shell character prior to doping and this character was retained after doping. This highlights the important point that the radical site from the galvinoxyl system is interacting with the PCQ chain in such a manner that it is not disrupting the open-shell component of the PCQ, which allows for two means by which to achieve the relatively high electrical conductivity value (~0.3 S cm^{-1}) shown in Figure 20a. We note that the electrical conductivity of the composite system increased relatively rapidly until a galvinoxyl radical loading of ~8% (by weight), which corresponds to the emergence of reflections associated with crystalline domains of the galvinoxyl radical in the powder wide-angle X-ray scattering data although these (presumably small) domains are not visible in atomic force microscopy (AFM) images. Thus, it is likely that the galvinoxyl radical is reaching a point where

it is phase separating from the PCQ matrix; this phase separation, in turn, limits the level of doping that can be achieved through the open-shell small molecule. Conversely, this also means that it may be possible to increase the electrical conductivity of the system to an even higher level if this phase separation could be mitigated and the polymer and dopant could remain molecularly mixed.

While the electrical conductivity for the blend systems saw an ~100-fold increase, the Seebeck coefficient only decreased by a factor of ~2 across the entire loading of galvinoxyl radical (Figure 20b). This ability of radical dopants to alter the electrical conductivity in a rather significant manner while only slightly altering the Seebeck coefficient is consistent with our data for P3HT reported above. However, the relatively large magnitude of the undoped PCQ Seebeck coefficient (i.e., > 1 mV K^{-1}) and the ability of the dopant to keep this Seebeck coefficient at > 600 μV K^{-1} at the highest-performing galvinoxyl loading (i.e., 10%, by weight) is of significant note. In turn, this results in an optimized power factor of > 10 μW m^{-1} K^{-2}, which is one of the larger values reported for non-PEDOT:PSS polymer thermoelectric systems. In fact, these relatively large Seebeck coefficient values point to a clear path forward for the next-generation of thermoelectric polymer materials, based upon radical-containing macromolecules, if the electrical conductivity of these materials could be increased in a cleverly designed manner. Therefore, we anticipate that this design archetype of combining radical-containing polymers with open-shell dopants will lead to significant strides in polymer thermoelectric materials and devices.

Importantly, these results highlight the potential to access narrow band gap DA copolymers with open-shell character using straightforward synthetic approaches, and importantly, they demonstrate alternative polymer-small molecule interactions relative to conventional doping to impart electrical conductivity and promising thermoelectric properties in CPs. The addition of an open-shell galvinoxyl radical dopant significantly increases the electrical conductivity while minimally impacting the Seebeck coefficient. In turn, this allows for the systematic optimization of the thermoelectric performance, resulting in an optimized power factor of > 10 μW m^{-1} K^{-2}, one of the larger values reported for non-traditional CP thermoelectric systems. This combination of a radical-containing macromolecule with an open-shell small molecule dopant opens a new pathway by which to control charge transport and enable unique transport behaviors in next-generation thermoelectric polymer systems.

Conclusions and Brief Outlook

In this effort, our team has been able to significantly advance the organic and physical chemistry associated with optoelectronically-active and thermoelectric polymers that interact with open-shell species. In this way, we have been able to establish the fundamental underpinnings of a new field of research, and we have utilized these advances in fundamental science in order to generate materials with never-before-observed (and never-before-predicted) properties. In this way, we believe that we have made a substantial impact with respect to both the relevant academic communities and with agencies with the defense community. In turn, we envision that this work can serve as a launching point for new scientific fields and for a means by which to translate the results of this work into systems that will provide strategic advantages to the warfighter as well. Importantly, we anticipate these results will be of weighty utility as our team and others move forward with respect to the development of spin-based soft materials systems, which is a promising new frontier in organic electronics research.